6. PAVEMENT RESPONSE

6.1. Introduction

The third major topic of this thesis is pavement response, and in particular transient response of pavement structures to moving loads. In Section 2.5 a number of issues around pavement structure response were identified. The purpose of Section 2.5 was mainly to determine the current best available knowledge and the current needs for developments and improvements.

The objective of this chapter is to evaluate two pavement response procedures and indicate the nominal differences between static and transient pavement response parameters. Transient response is defined as the response of a pavement to a moving load input. The effects of vehicle speed, pavement mass inertia and damping on pavement response are included in a transient analysis.

The focus in this chapter is on the response of three specific pavement structures to the tyre loads developed in Chapter 5. Only linear elastic material models are used for the response analyses, and existing transfer functions from the South African Mechanistic Design Method (SAMDM) (Theyse et al, 1996) are used to evaluate the expected lives calculated from the different analysis methods. Development of improved material models and transfer functions are explicitly excluded from this thesis (see Section 4.5.3).

Although there are only three basic pavement structures used for the analyses in this thesis (refer to Table 2.8 and Sections 2.6.3 and 4.6.2), two of these pavement structures (the national and provincial pavements) incorporate lightly cemented layers in their structures. These materials change to an equivalent granular state relatively early in their lives. This changes the properties of the materials. To calculate realistic pavement responses and lives, these two pavement structures are evaluated in both a cemented (suffix ***cem***) and equivalent granular (suffix ***eg***) state in this chapter. This cause the analyses to be performed on five pavement structures, although the pavement lives are combined in the end to provide only a pavement life for each of the three nominal pavement structures. To expedite analyses and contain the amount of data for analysis, only the first (fully cemented) and the final (fully equivalent granular state) phases of the provincial pavement's life were analysed.

The chapter is structured into a static response analysis and a transient response analysis. In each of these sections the primary results of the specific analysis are discussed together with inferences based on the specific data. In Section 6.4 the data from the analyses are compared. In Section 6.5 a method is developed for converting between static and moving pavement response parameters.

6.2. Static Response Analysis

6.2.1. Introduction

Static linear elastic pavement structure response analysis is defined, for the purposes of this thesis, as the calculation of stresses, strains and deflections in a pavement, caused by a time-independent tyre load that is fixed at one location. The stresses, strains and deflections are related to the applied tyre load through a linear elastic material model. This type of analysis is termed static response analysis in the remainder of this thesis.

The objective of this section is to obtain the pavement responses and expected lives that would normally be obtained using the procedures typically used in South Africa. The loads used consist of static loads distributed over circular areas of uniform contact stresses. The pavement structure is defined in terms of layer thicknesses, material stiffnesses and Poisson ratios. The pavement response is converted to expected pavement lives using the SAMDM transfer functions (Theyse et al, 1996).

The tyre loads used originate from the tyre load distribution obtained from evaluating all the static tyre loads of all three the vehicles at the three load conditions defined in Chapter 5. The specific loads are shown in Tables 5.5 and 6.1. Tyre loads at the 50^{th}, 80^{th}, 90^{th} and 95^{th} percentile values are used as input data. The correspondent axle load (assuming a single axle with dual tyres) and equivalent 80 kN load (assuming an exponent of 4,0) for each of the load cases are also shown in Table 6.1. The pavement structures for which the analyses were performed are shown in Tables 4.4 and 6.2. The material properties used for each of the layers are shown in Table 4.5.

Table 6.1: Selected tyre loads (single tyre) for static response analysis.

	50^{th} percentile	80^{th} percentile	90^{th} percentile	95^{th} percentile
Tyre Load [kN]	21,3	23,8	24,4	33,6
Axle Load [kN]	85,2	95,2	97,6	134,4
E80 (n=4,0)	1,3	2,0	2,2	8,0

Table 6.2: Layer thicknesses for three pavement structures analysed in this thesis (from TRH4 (1996).

Layer	National road structure	Provincial road structure	Rural road structure
Surfacing	50 mm Asphalt	Double seal	Double seal
Base	150 mm G1	125 mm C3	125 mm G4
Subbase	300 mm C3	152 mm C4	125 mm G6
Subgrade	500 mm SG1	500 mm SG1	500 mm SG1

The stress, strain and deflection responses from the pavement structures were evaluated using the ELSYM5M (ELSYM5M, 1995) and SAMDM (Theyse and Muthen, 2000) software. Both these methods use the ELSYM engine, but the SAMDM procedure also calculates the expected lives of the various layers and the pavement structure.

The load case used for all the analyses consisted of a single tyre load applied to the pavement structure. This was done to enable direct comparison with the responses calculated using the axi-symmetric finite element software (Section 6.3). In the remainder of this section the pavement responses calculated and expected lives for each of the pavement structures and load cases are discussed. These results are compared to those obtained from the other analysis method in Section 6.4.

6.2.2. Pavement response from static response analysis

The data obtained from the static response analyses consist of stresses, strains and deflections at various locations in the pavement structure. These locations were based on the critical positions in the pavement structure for each parameter.

The deflection responses were calculated on the surface of the pavement structure, at distances from the centre of the tyre load shown in Table 6.3. The stress and strain responses were calculated at the centre of the tyre load at depths indicated in Table 6.4. These distances and depths coincided with the layer interfaces and the mesh selected for the axi-symmetric finite element analyses. The shear stresses and strains were calculated under the edge of the tyre. The maximum pavement response values for the static response analyses are shown in Table 6.5.

Table 6.3: Positions at which elastic surface deflections were calculated for each pavement structure.

	National road structure	Provincial road structure	Rural road structure
Distance from centre of tyre load [mm]	0 mm	0 mm	
	102 mm	102 mm	
	305 mm	279 mm	
	762 mm	787 mm	
	2 921 mm	2 057 mm	

Table 6.4: Depths at which stresses and strains were calculated for each pavement structure.

	National road structure	Provincial road structure	Rural road structure
Depth below centre of tyre load [mm]	0 mm	0 mm	0 mm
	51 mm	76 mm	63 mm
	127 mm	127 mm	127 mm
	203 mm	203 mm	190 mm
	508 mm	279 mm	250 mm

Table 6.5: Maximum stresses, strains and deflections calculated for each pavement structure.

Parameter	National road structure[1]	Provincial road structure[1]	Rural road structure
Maximum elastic surface deflection [mm]	0,32 (0,41) surface	0,28 (0,79) surface	0,57 surface
Vertical compressive strain [με]	948 (897) centre G1	2 058 (268) centre EG3	920 bottom G4
Horizontal tensile strain [με]	397 (421) bottom AC	141 bottom C4 (817) centre EG4	465 bottom G4
Vertical compressive stress [kPa]	1 069 (1 069) surface	1 069 (1 069) surface	1 069 surface
Horizontal compressive stress [kPa]	2 523 (2 978) surface	1 298 (1 104) surface	1 355 surface
Shear compressive stress [kPa]	55 (67) surface	148 (85) centre of C3/EG3	165 centre of G4

1 Values for equivalent granular state shown in brackets.

Analysis of the results of the pavement structure response calculations indicated the following (all responses indicated below the centre of the loaded area except for the shear parameters which were located at the edge of the loaded area). These responses are as would be expected from existing pavement analysis knowledge, but are emphasised here to indicate that the analysis method and parameters caused responses normally expected from these conditions:

Elastic surface deflection

The trends observed in the data for each pavement structure (regardless of applied load percentile) were similar for the specific pavement. The higher percentile loads caused deeper deflections than the lower percentile loads. Typical elastic deflection bowls for each of the pavements at the 50th load percentile are shown in Figure 6.1. The rural, national ***eg*** and provincial ***eg*** structures had higher elastic deflections close to the loaded areas than the national ***cem*** and provincial ***cem*** pavement structures. This may be attributed to the high stiffness cemented layers (national ***cem*** and provincial ***cem*** pavements) as well as the high stiffness asphalt surfacing (national pavement). Similar deflection values were calculated further than 500 mm from the centre of the load for all pavement structures. These similar deflections were caused by the same subgrade used for all the pavement structures in the analyses.

Vertical elastic strain

Similar trends were observed in the vertical strains calculated for each pavement structure, regardless of applied load percentile. Typical vertical strains for each of the pavement structures are shown in Figure 6.2 at the 50th load percentile. Compressive strains were calculated at all depths except the surface. The tensile surface strains calculated on the surface is probably due to a modelling effect, and is generally found for these types of analyses. The provincial ***eg*** pavement yielded a compressive vertical strain on the surface as well as the highest overall strain value. The provincial pavement ***cem*** yielded the lowest vertical strains due to the presence of two lightly cemented layers in the pavement structure. The major difference between the provincial pavement structure response in the cemented and the equivalent granular phases is the large difference in elastic modulus before and after cracking (decrease from 2 000 MPa to 400 MPa. The responses from the rural and national (***cem*** and ***eg***) pavements were similar, due to the presence of granular layers in both these pavements.

Horizontal elastic strain

Each of the pavement structures yielded similar trends for the calculated horizontal strains at the depths investigated at all load percentiles. The higher load percentiles yielded higher strains. Tensile strains were calculated at all depths except on the surface. Typical trends for each of the pavements are shown in Figure 6.3. The highest horizontal strains were calculated in the provincial ***eg*** pavement, with the provincial ***cem*** pavement exhibiting the lowest horizontal tensile strains. The horizontal strains were mainly influenced by the elastic stiffnesses of the materials.

Vertical stress

Vertical compressive stresses calculated for the various pavement structures showed similar trends for all the pavements at all load percentiles (Figure 6.4). The calculated stresses at the surface correlated exactly with the applied uniform contact stresses. Stresses decreased with depth in the pavement, and increased with increased load magnitudes.

Horizontal stress

The horizontal stresses calculated for the various pavement structures showed similar trends (Figure 6.5), except for the national (***cem*** and ***eg***) pavements. The rural and provincial pavements (***cem*** and ***eg***) showed tensile stresses at depths of deeper than 130 mm, while the national pavements (***cem*** and ***eg***) showed tensile stresses at a depth of 50 mm. Tensile stresses cannot be generated in granular layers. However, this is a phenomenon previously shown to occur when analysing a granular pavement using linear elastic theory (Theyse et al, 1996).

Shear stress

The shear stresses calculated for the rural and provincial (***cem*** and ***eg***) pavement structures showed similar trends (Figure 6.6). Higher shear stresses were calculated in the centre of the base layer, with lower stresses at deeper locations in the pavements. The national (***cem*** en ***eg***) pavements showed a different trend with a lack of the high shear stresses in the base layer. This may be attributed to the thicker and stiffer asphalt surfacing used for these pavements.

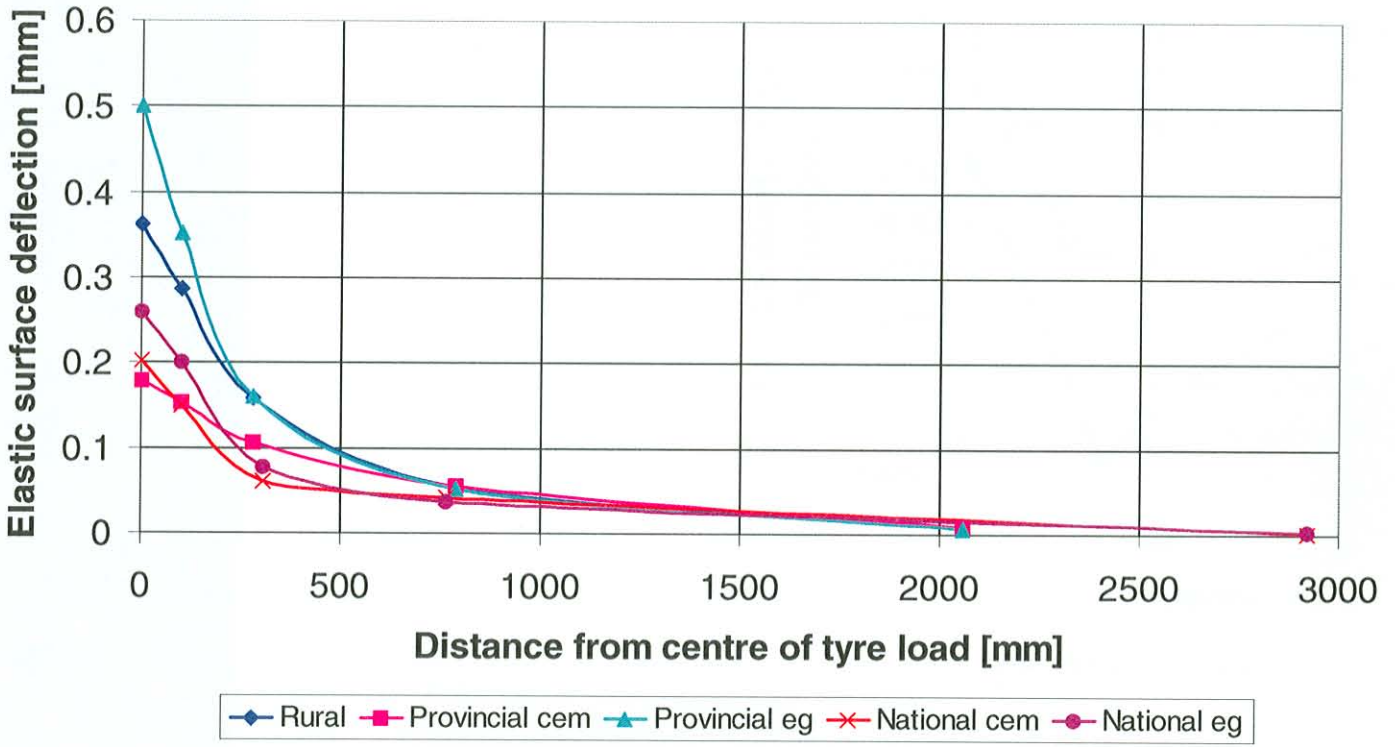

Figure 6.1: **Typical elastic surface deflection data (under centre of load) for pavements evaluated using 50th percentile static load.**

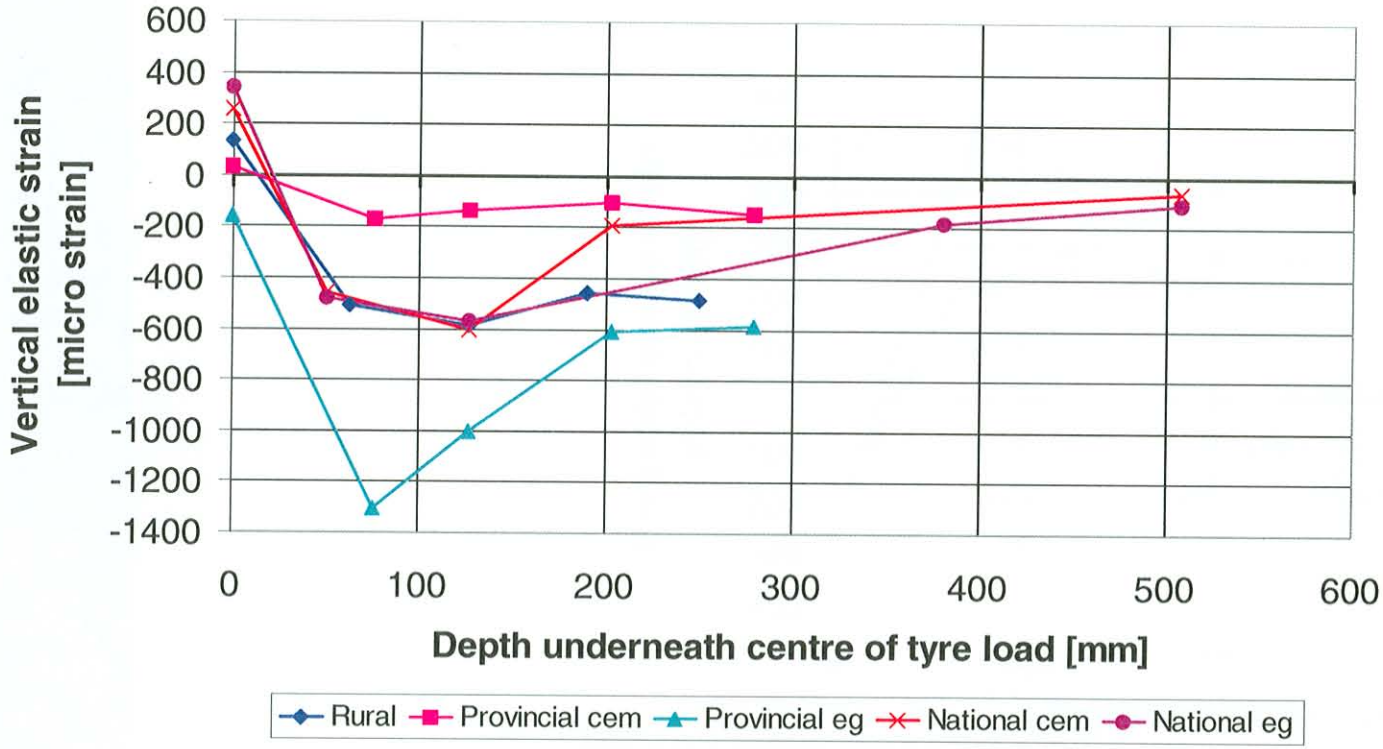

Figure 6.2: **Typical vertical strain data (under centre of load) for pavements evaluated using 50th percentile static load.**

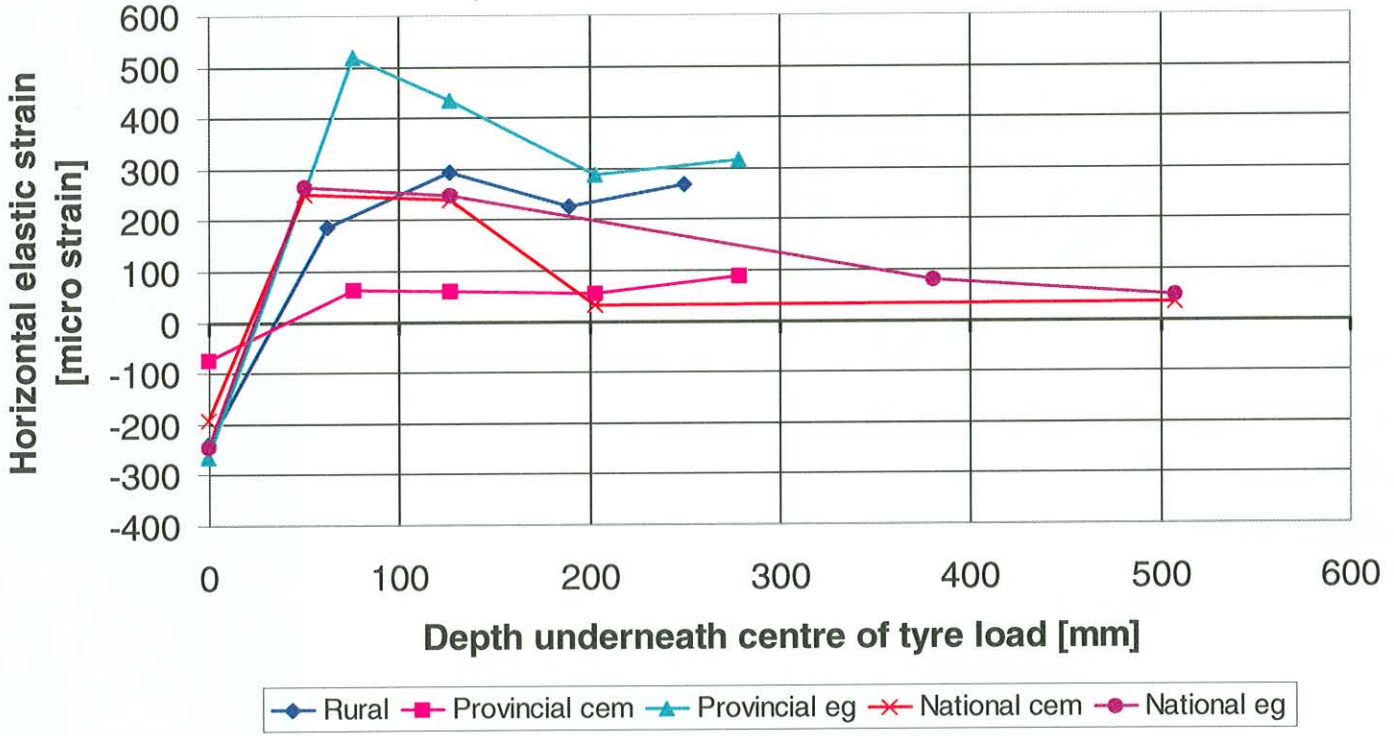

Figure 6.3: **Typical horizontal tensile strain data (under centre of load) for pavements evaluated using 50th percentile static load.**

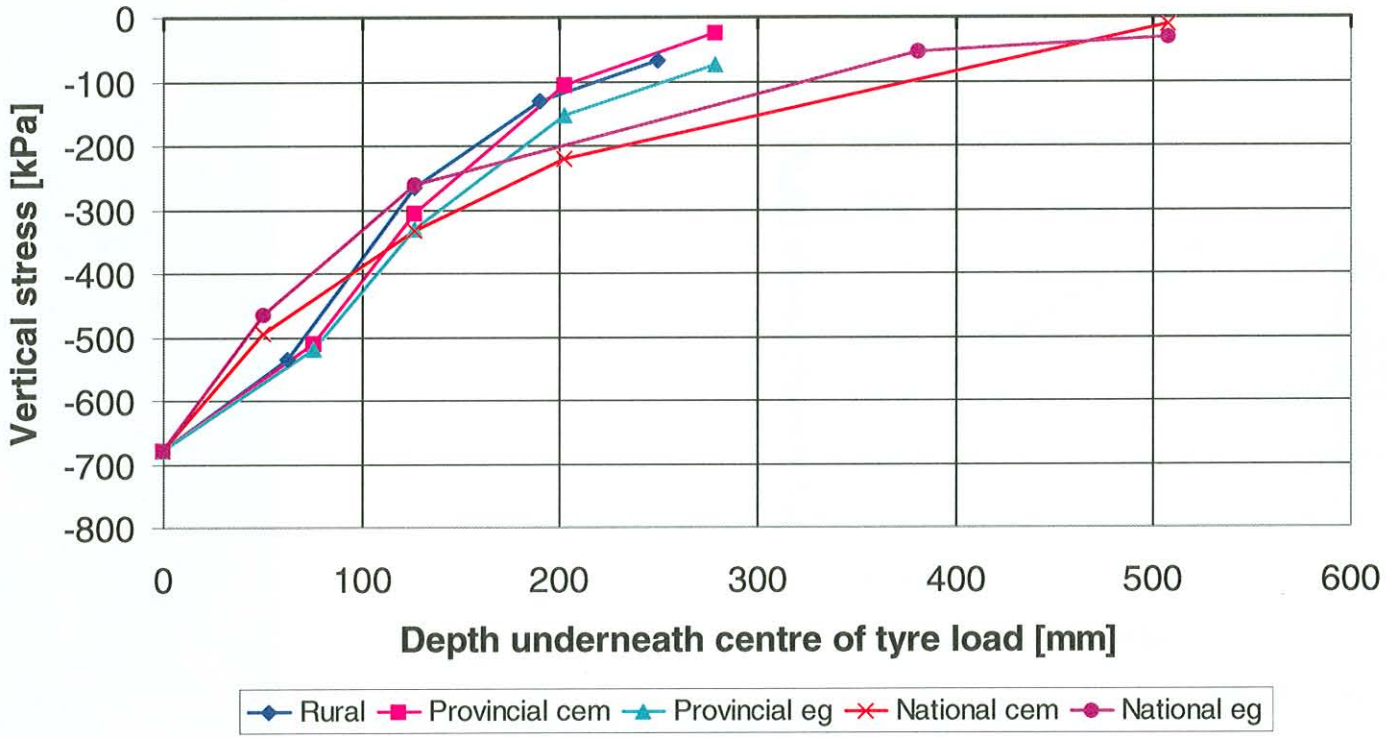

Figure 6.4: **Typical vertical stress data (under centre of load) for pavements evaluated using 50th percentile static load.**

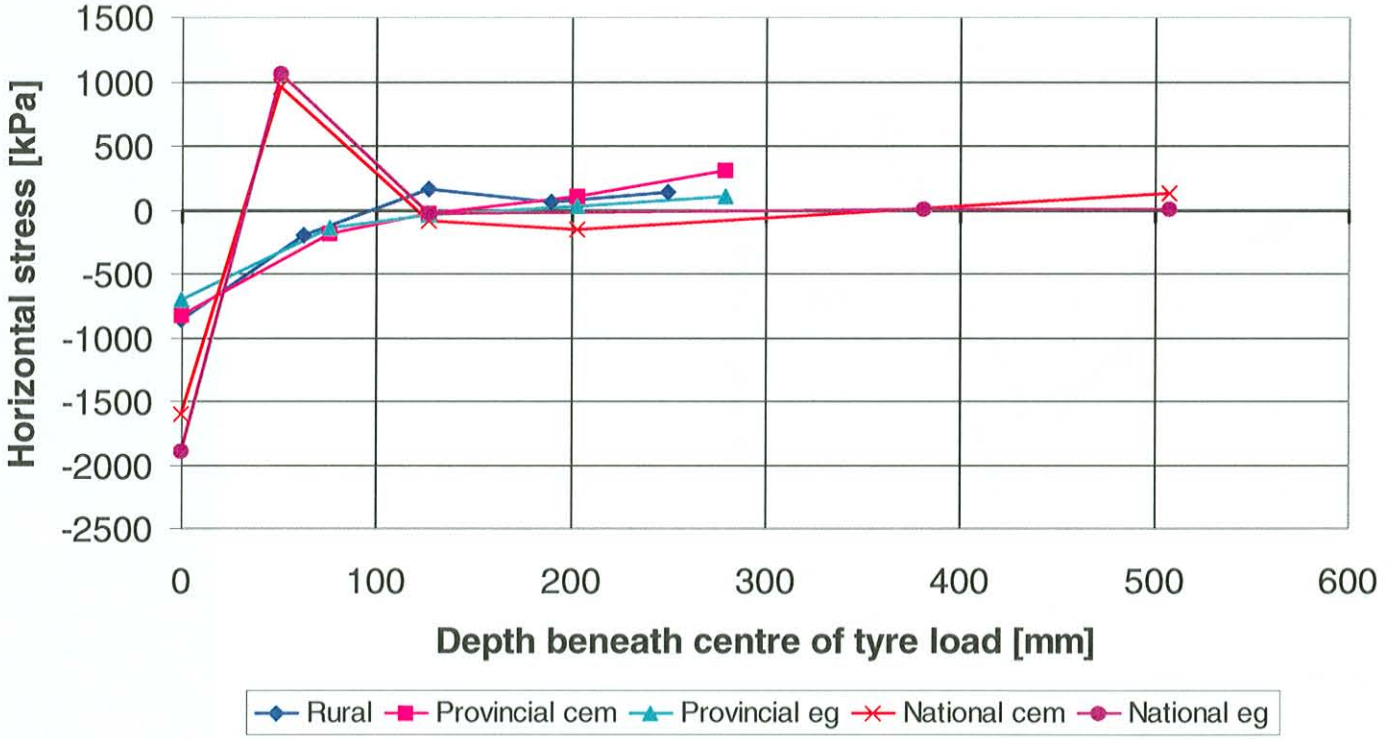

Figure 6.5: Typical horizontal stress data (under centre of load) for pavements evaluated using 50th percentile static load.

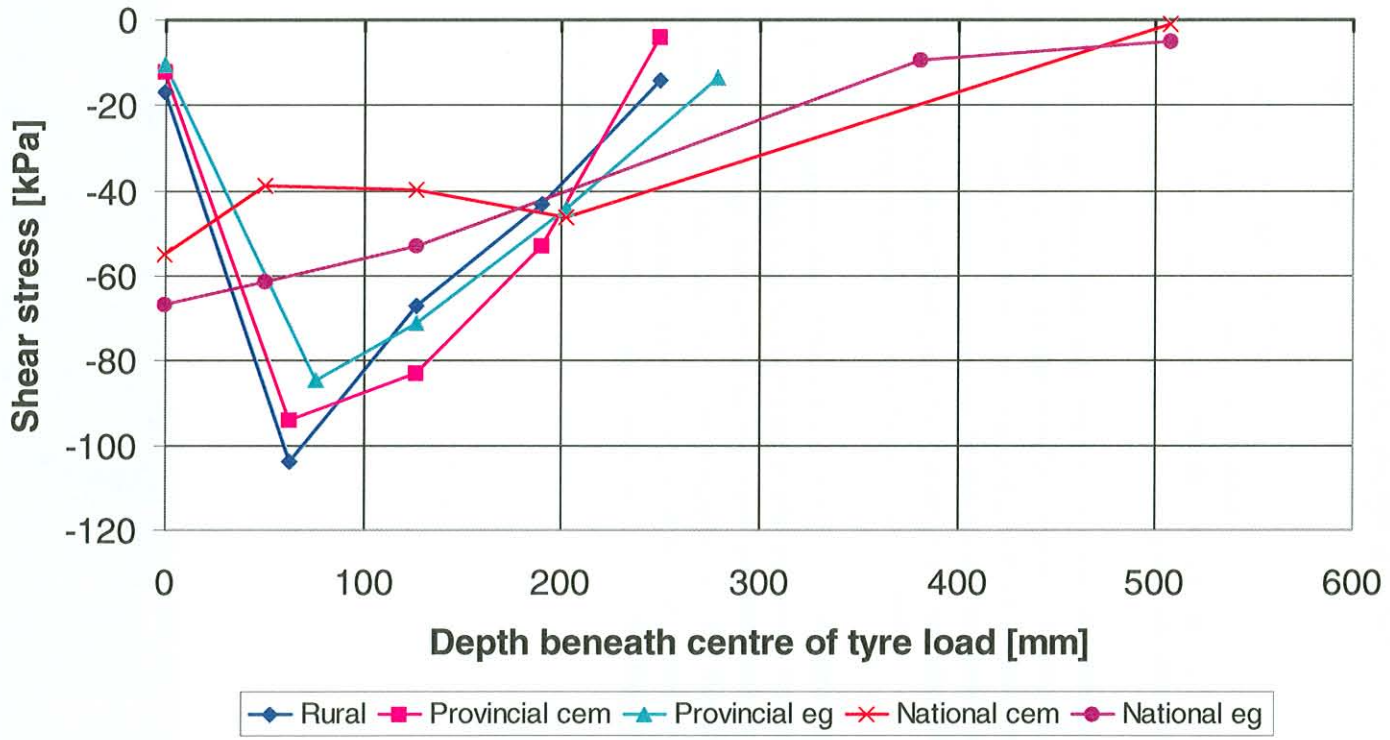

Figure 6.6: Typical shear stress data (under edge of load) for pavements evaluated using 50th percentile static load.

Ratios

The ratios between stresses, strains and deflections calculated at the four different load percentiles were evaluated to determine whether the changes in load magnitude caused similar changes in response. Similar patterns were found for all the pavements and parameters. The ratios between pavement response parameters for the four tyre load percentiles are shown in Table 6. 6. The ratios for the four load cases are also shown. The similar patterns evolve from the strong load dependence of the pavement response parameters shown in the statistical analyses.

Table 6.6: Ratios between tyre loads and pavement response parameters (stresses, strains and deflections) for static response analyses.

Load percentile [%]	Tyre load [kN]	Tyre load ratio	Pavement response parameter[a] ratio
50	21,3	1,00	1,00
80	23,8	1,12	1,12
90	24,4	1,15	1,15
95	33,6	1,58	1,58

a - stresses, strains and deflections

Statistical analysis

A statistical analysis between the calculated pavement response parameters and applied tyre loads confirmed the direct relationship between applied load and calculated response at all depths and positions.

6.2.3. Expected pavement lives

The stresses, strains and deflections discussed in Section 6.2.2 were used to calculate the expected pavement lives for each of the different load scenarios, using the SAMDM transfer functions. A summary of the critical lives in each pavement structure is shown in Table 6.7.

When these calculated expected lives are compared with the design traffic indicated in the design catalogue (TRH4) for the specific pavement structures, the calculated pavement classes (ES3 and ES0,3) for the rural and provincial pavements are similar to the design classes. The calculated expected life for the national pavement structure is higher than the design class shown in TRH4, but within the range of lives calculated for the specific pavement structure during the development of TRH4 (Theyse, 2000).

The critical expected lives indicated in Table 6.7 are all calculated under the 95th percentile load, as higher loads generally cause shorter pavement lives using the SAMDM transfer functions (although the norm is to use lower percentile values for rural roads, the same percentile values were used for all the comparisons in this thesis). The data indicate that the expected lives of the three pavements decreased with increased load percentiles. This is to be expected, as the stresses and strains used to calculate the expected lives from, increased with increased loads.

Table 6.7: Summary of critical expected pavement lives based on ELSYM analyses and SAMDM transfer functions.

Pavement structure (design traffic class)	Critical layer	Average expected life [million E80s] (traffic class)	Average total expected life [million E80s] (traffic class)
National (ES100)	C3	2,5 (ES3)	140 (ES100+)
National (equivalent granular)	G1	137 (ES100+)	
Provincial (ES3)	C4	1,2 (ES3)	1,2 (ES3)
Provincial (equivalent granular)	EG5	0,88 (ES1)	
Rural (ES0,3)	G6	0,01 (ES0,03)	0,01 (ES0,03)

6.2.4. Summary of static pavement response analyses

The results from the static pavement response analyses indicate that similar trends can be expected from the various pavement response parameters for each of the pavement structures investigated at the various tyre load percentiles. Increased load magnitude (percentile) resulted in increased stresses, strains and deflections. A perfect linear relationship exists between the load magnitudes and the calculated pavement response parameters. The applied loads influence the expected lives of the various layers in the pavements critically.

6.3. Transient Response Analysis

6.3.1. Introduction

The transient response analysis was performed as the advanced pavement response analysis tool using two finite element methods. It involved a 2-dimensional axi-symmetric package (Jooste, 1999). Attempts were made to also use a 3-dimensional finite element package to evaluate the transient response of a pavement as loaded by a set of moving dynamic loads, representing a full vehicle. However, it proved to be technically complicated, and was therefore left out of this thesis. Issues around performance of 3-dimensional MDL analyses and the expected results thereof are, however, addressed in Section 7.4. There are also recommendations made towards performing such an analysis.

All the load cases were analysed using the 2-dimensional method. The 2-dimensional analysis involved a Moving Constant Load (MCL) analysis. The 2-dimensional analysis involved a load that moved but did not change load magnitude (see Section 4.2.2 and 4.2.3 for detailed definitions). The term transient response analysis is used in this thesis for the finite element analysis.

Only the data for the left wheeltrack steering tyre were used. This was to enable comparison with the data obtained from the static response analysis. In this process exact tyre loads (as opposed to equivalent tyre loads from dual tyre sets) were used for the analyses.

The inferences drawn from the load cases analysed using only the MCL method focus only on the transient response of the pavement to a single tyre load. It is recommended that these load cases be analysed using a 3-dimensional approach when the costs are within a specific project's scope.

The tyre loads used for the MCL analyses originate from the tyre load distribution obtained from evaluating all the moving tyre loads of all three vehicles at the three load conditions defined in Chapter 5. The specific loads are shown in Tables 5.6 and 6.8. Tyre loads at the 50^{th}, 80^{th}, 90^{th} and 95^{th} percentile values are used as input data. The correspondent axle load (assuming a single axle with dual tyres) and equivalent 80 kN load (assuming an exponent of 4,0) for each of the load cases are shown in Table 6.8. The difference between the tyre loads in Table 6.8 and the static tyre loads in Table 6.1 is that the tyre loads in Table 6.1 were measured while the vehicles were standing still, while those in Table 6.8 were measured while the vehicles were moving.

Table 6.8: Selected tyre loads for intermediate pavement response analysis (based on DADS generated tyre loads).

	50^{th} percentile	80^{th} percentile	90^{th} percentile	95^{th} percentile
Tyre Load [kN]	24,0	30,9	33,3	34,7
Axle Load [kN]	96,0	123,6	133,2	138,8
E80 (n=4,0)	2,1	5,7	7,7	9,1

The pavement structures on which the analyses were performed are shown in Tables 4.4 and 6.2. The material properties used for each of the layers are shown in Table 4.5. The national and provincial road structures (which include cemented layers) were again evaluated using two phases (a cemented and equivalent granular phase).

The asphalt surfacing stiffness (2 980 MPa) shown in Table 4.5 was used as the static stiffness (elastic modulus) of the asphalt surfacing on the national pavement structures. The Asphalt Institute Formulas for calculating dynamic modulus of asphalt layers, as referenced by Huang (1993), were used to calculate the dynamic asphalt modulus at the speeds at which the pavement response analyses were performed. The calculated stiffnesses at the indicated speeds are shown in Table 6.9.

Table 6.9: Calculated dynamic stiffnesses for asphalt surfacing of national pavements using Asphalt Institute formulas.

Load speed [km/h]	40	60	80	90	100
Dynamic stiffness [MPa]	5 568	6 588	7 611	8 138	8 681

A linear elastic material model was used for the transient response analysis method. The reasons for this decision were to enable direct comparison with the current standard pavement response analysis (static response analysis using ELSYM5M), to keep the variables between the two pavement response analysis methods to a minimum, and because an investigation into the non-linear response of pavements to loads is outside the scope of this thesis (see Section 4.5.3). However, this does not mean that the aspect of non-linear material response is trivial or not important. The additional value of doing a non-linear material response analysis will mainly lie in a more realistic representation of the response of the pavement to loading, especially in terms of permanent deformation. The additional cost of this exercise (in terms of additional input parameters, longer response calculation times and more complicated data reduction and analysis techniques) must also be accounted for. Further, the current SAMDM transfer functions only make provision for pavement responses calculated using linear elastic material response parameters.

The meshes used for each of the three pavements in the MCL analyses consisted of between 100 (rural and provincial pavements) and 130 (national pavement) elements. Each of these 2-dimensional meshes was 4 064 mm wide and 4 064 mm deep, and was constrained at its edges. The smallest elements were 25,4 mm x 25,4 mm in size. These elements were located underneath the applied load.

The process used to calculate the pavement response under a moving tyre load consisted of applying the tyre loads at fixed positions on the pavement surface, and monitoring of the pavement responses at positions in the pavement equivalent to the distance from the loaded areas at the required speed.

The MCL analyses were performed using an axi-symmetric finite element package (Owen and Hinton, 1980). The load was applied to the pavement as a sinusoidal pattern that was applied for a time equivalent to the time required to cover the tyre patch area (assumed as a 200 mm diameter circle) at the speed for which the analysis was performed. The pavement responses were then monitored at various nodes on the mesh at times equivalent to the time for the tyre load to travel the distance at the speed at which the analysis was performed. This method caused the response of the pavement to be equivalent to that for a pavement over which the load is moving. The concept is shown schematically in Figure 6.7.

The time required to move between two nodes on the finite element mesh at the analysis speed was used to decide which of the time steps' data at a specific position should be used in the calculation.

The pavement responses were monitored at specific depths in the pavement. These depths coincided with interfaces between layers as well as the positions at which stresses and strains are required in the SAMDM analyses. The specific depths at which pavement response was monitored for each of the pavements are shown in Table 6.10. As the positions for the MCL analyses coincided with Gauss points in the elements, they are not similar to the positions of the mesh nodes.

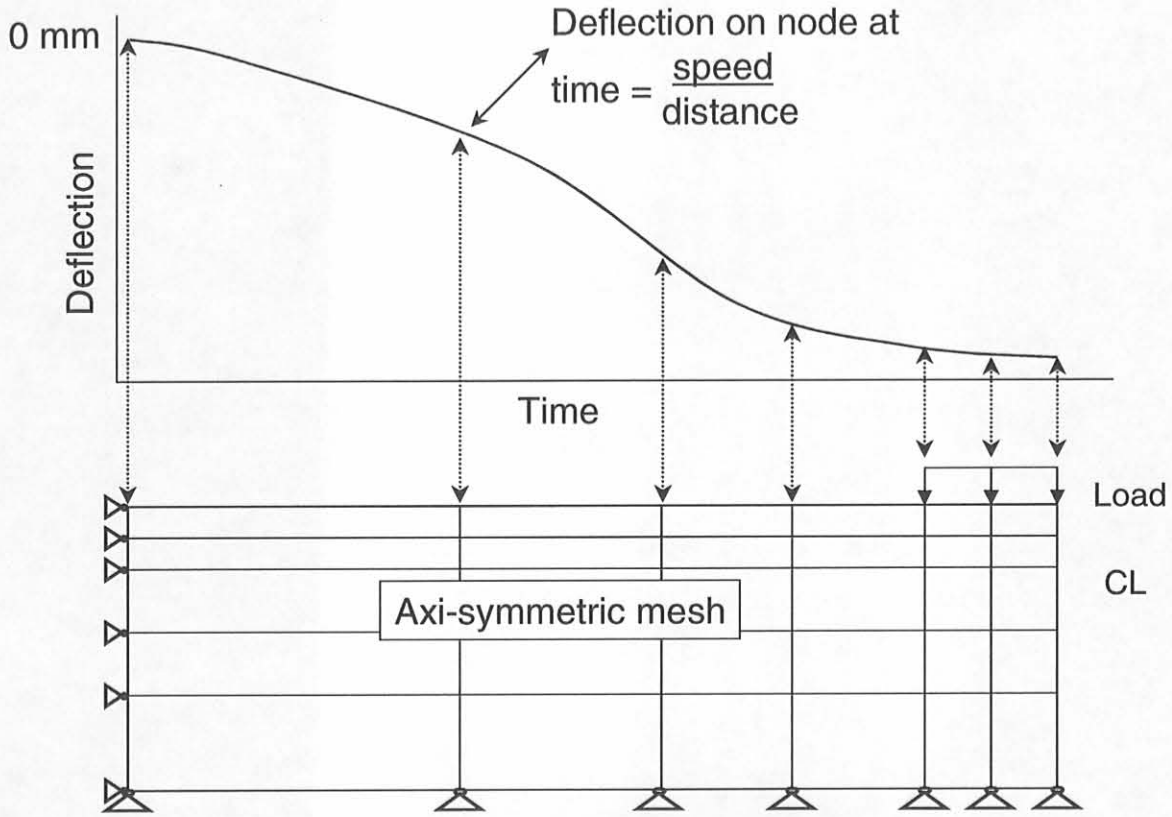

Figure 6.7: **Graphical explanation of development of deflection bowls from axi-symmetric finite element data using superposition method.**

Table 6.10 Depths at which stresses and strains were calculated for each pavement structure.

	National road structure	Provincial road structure	Rural road structure
Depth below centre of tyre load [mm]	7 mm	7 mm	7 mm
	42 mm	58 mm	58 mm
	58 mm	91 mm	91 mm
	109 mm	109 mm	109 mm
	211 mm	152 mm	147 mm
	348 mm	178 mm	170 mm
	414 mm	229 mm	211 mm
	450 mm	254 mm	234 mm
	567 mm	363 mm	338 mm

6.3.2. Analyses output

The results from the MCL analyses are shown and discussed in this section. In Section 6.4 these results are compared with results from the static response analyses.

The standard outputs from the MCL analyses are vertical deflection, vertical, horizontal and shear stresses and vertical, horizontal and shear strains. Figures 6.8 to 6.22 show the maximum values of the pavement response parameters at the indicated depth for the 50th percentile load case. It also shows changes with time for the stresses calculated. The strains were not calculated directly in the software, but at selected positions and time intervals and are therefore not plotted against load time. The figures of stress against time are for the rural pavement with a 95th percentile load. The actual load duration time is also indicated. The last set of figures indicates the change in response parameters against speed.

Elastic vertical deflection

A typical relationship between elastic vertical deflection and load speed for the range of pavement structures is shown in Figure 6.8. The elastic surface deflections calculated decreased with increased load speed and increased with increased load magnitude. The major part of the decrease related to load speed occurs before a load speed of 40 km/h is reached. At higher load speeds the decrease is less prevalent. This phenomenon was measured by Lourens (1995) and it appears that most of the reduction occurs at speeds lower than 40 km/h. This was, however, outside the range of speeds investigated in this thesis.

The elastic vertical deflection values ranged between 0,18 mm and 0,50 mm for static loads, while the values ranged between 0,03 mm and 0,12 mm at load speeds of 100 km/h. The highest deflection was calculated for the provincial ***eg***, rural and national ***eg*** pavements, which contained only granular layers in their structures. In Figure 6.9 typical deflection bowls at 40 km/h and 100 km/h are shown for the provincial pavement. The phase difference in the position of the maximum deflection is apparent from the figure. The difference in maximum deflection at the two speeds is also visible. The staggered shape of the graphs is due to the

superposition method used to develop the moving load deflection bowls from the axi-symmetric finite element method results (as discussed earlier).

Vertical stress

A typical relationship between vertical stress and load speed for the range of pavement structures is shown in Figure 6.10. Similar trends were observed at all load magnitudes. Compressive vertical stresses were calculated in all layers of the pavement structures. The vertical stresses at the surface of the pavement correlated well with the applied load pressures. Vertical stresses decreased with increasing depths except for the national ***cem*** and ***eg*** pavements. Higher vertical stresses were calculated at the bottom of the relative stiff asphalt surfacing. Vertical stresses decreased slightly with increasing load speeds for the national (***cem*** and ***eg***) and provincial (***cem*** and ***eg***) pavements (Figure 6.11). The vertical stresses for rural pavements increased again at speeds higher than 40 km/h. These increases in vertical stress with increased load speeds, correlates with the typical decreases in vertical elastic deflection with increased speeds. In Figure 6.12 typical vertical stress response with time as calculated from the MCL analyses are shown.

Horizontal stress

A typical relationship between horizontal stress and depth for the range of pavement structures is shown in Figure 6.13. Similar trends were observed in the data at all load percentiles. Compressive horizontal stresses were calculated in all layers of the pavement structures. The stress magnitude increased with increased applied tyre loads. The stress magnitudes were lower deeper into the pavement structure, and the rates of decrease in stress magnitude were also less dramatic at these depths. In Figure 6.14 the typical relation between the horizontal stress and speed is shown. These stresses decreased between 0 and 40 km/h, and remained relatively constant for further speed increases. In Figure 6.15 a typical horizontal stress response with time as calculated from the MCL analyses is shown.

Shear stress

A typical relationship between shear stress and depth for the range of pavement structures is shown in Figure 6.16. Similar trends were again observed at all load percentiles investigated. Compressive shear stresses were calculated in all layers. The stress magnitude increased with increased applied tyre loads. Stress magnitudes stayed relatively constant at speeds higher than 40 km/h (Figure 6.17). The national (***cem*** and ***eg***) and provincial ***eg*** pavements showed decreasing stresses between 0 and 40 km/h, while the stresses in the rural and provincial ***cem*** pavements remained relatively constant. The effect of load speed on stress magnitude was less dramatic than the effect of load magnitude. In Figure 6.18 a typical shear stress response with time as calculated from the MCL analyses is shown.

Horizontal strain

Typical horizontal strain responses against depth are shown in Figure 6.19 for the different pavement structures investigated. Similar trends were observed for all the load percentiles investigated. Tensile horizontal strains were calculated in all pavements analysed. These strains decreased with increasing depths. The provincial ***eg*** pavement yielded the highest strains in the upper 150 mm of the pavement. Similar trends were observed in the rural and provincial (***cem*** and ***eg***) pavements with decreasing strains at increasing depths. The national pavement (***cem*** and ***eg***) yielded lower horizontal strains at the surface than under the asphalt

surfacing and in the centre of the granular G1 base layer. This may be attributed to the very stiff asphalt surfacing incorporated in these pavements. In Figure 6.20 the horizontal strain is shown against increasing speed. The rural and provincial ***eg*** pavements showed increases in horizontal strain against increases in speed, while the strains for the other three pavements showed slight increases with increasing speeds. The maximum horizontal strains all changed from compressive strains to tensile strains with increases in speed.

Vertical strain

Typical vertical strain responses are shown in Figure 6.21. Similar trends were observed at all the load percentiles. The vertical strains for the rural and provincial pavements (***cem*** and ***eg***) decreased with increased depths. The national (***cem*** and ***eg***) pavements initially yielded increasing strains (through the asphalt surfacing layer) and deeper down in the pavement relatively constant strains. The initial increase in strain may be attributed to the effect of the stiff asphalt surfacing on calculated vertical strains. The provincial ***eg*** pavement yielded the highest vertical strains in the upper parts of the pavement (up to 150 mm). The vertical strains on top of the subgrades, from which the subgrade lives are calculated using the SAMDM transfer functions (Theyse et al, 1996) were similar for all pavements.

In Figure 6.22 the vertical strain is shown against increasing speed. All the pavements showed decreases in vertical strain with increases in speed. The provincial ***eg*** and rural pavements showed the highest compressive strains, with the national pavement (***cem*** and ***eg***) the lowest strains. The majority of the decrease in strain occurred between 0 and 40 km/h.

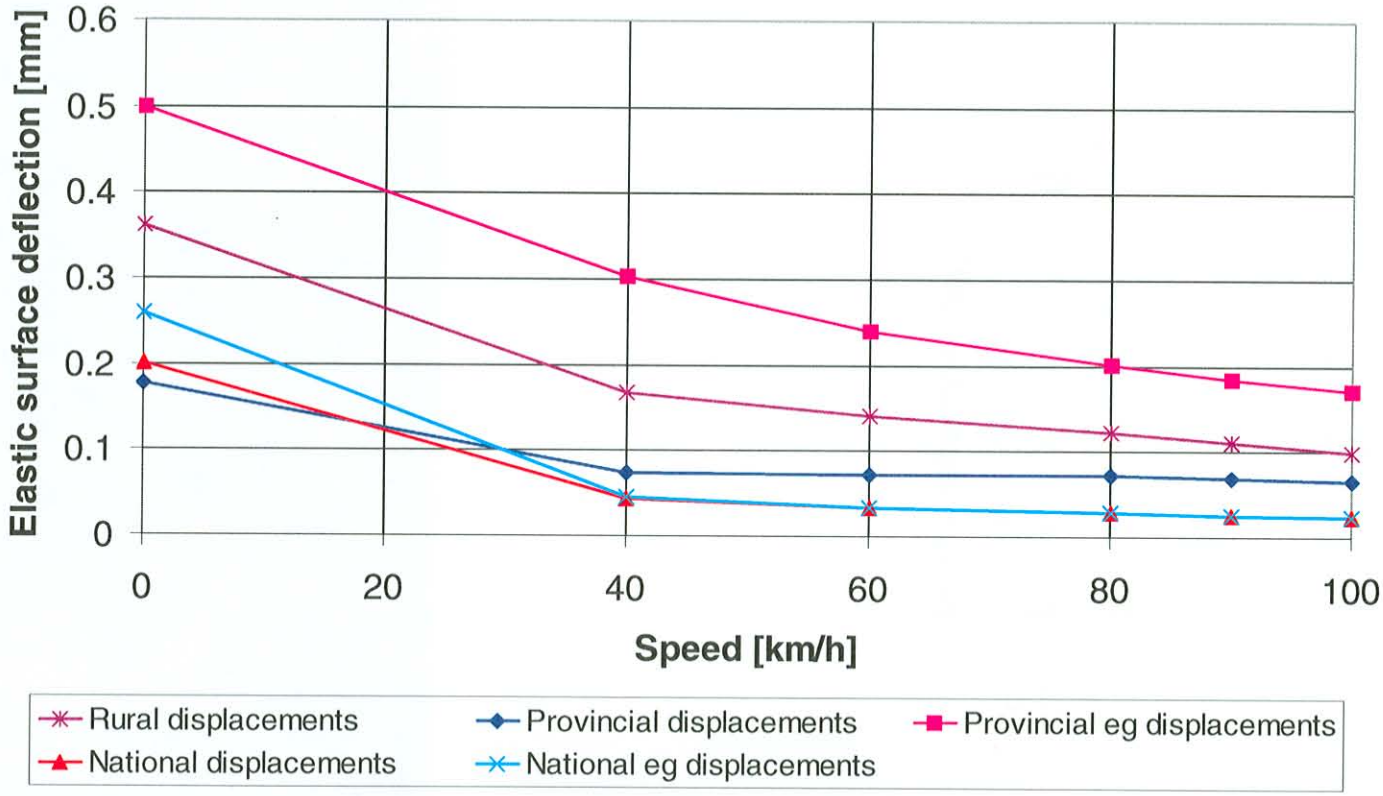

Figure 6.8: **Typical elastic surface deflections (50th percentile loads) as calculated using MCL method.**

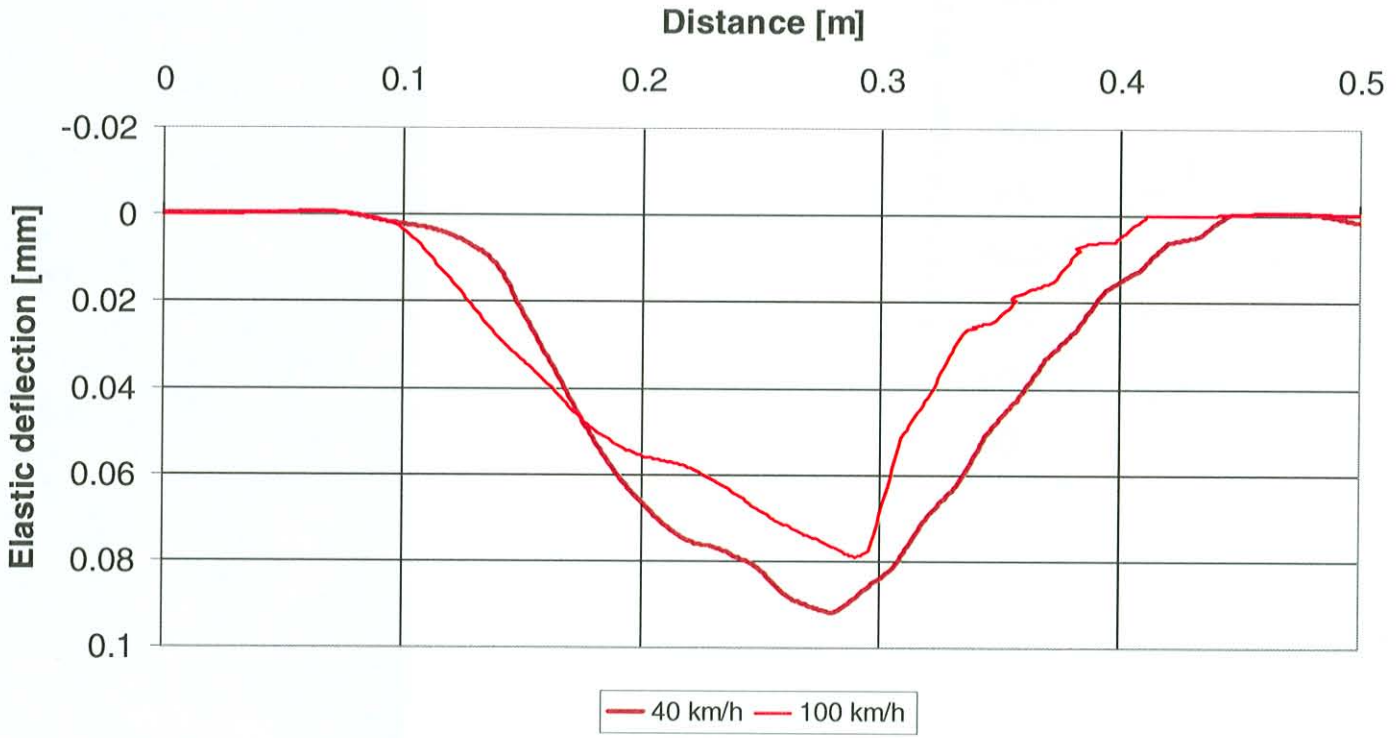

Figure 6.9: **Typical elastic surface deflection bowls (90th percentile loads) on provincial cemented pavement) as calculated using MCL method.**

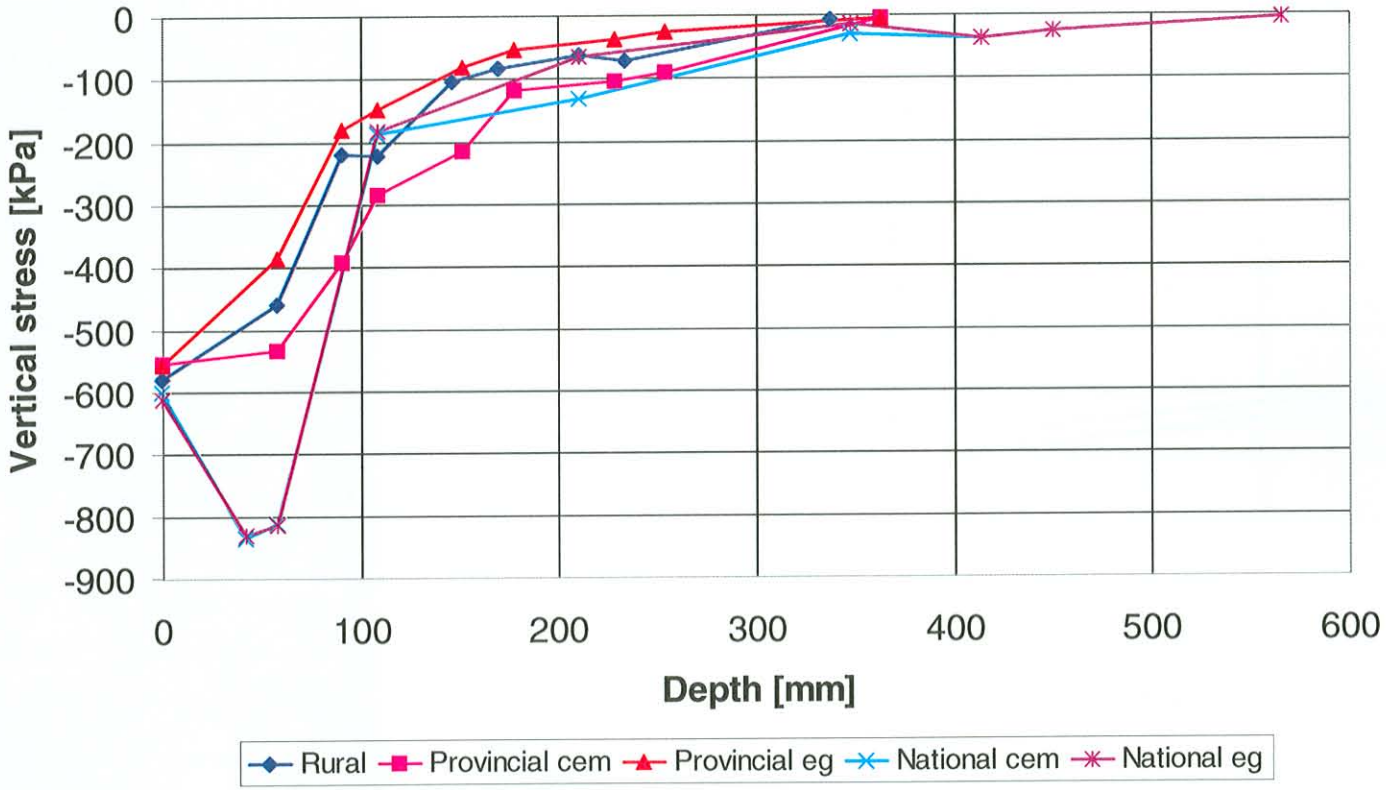

Figure 6.10: Typical vertical stresses (50th percentile load) as calculated using MCL method.

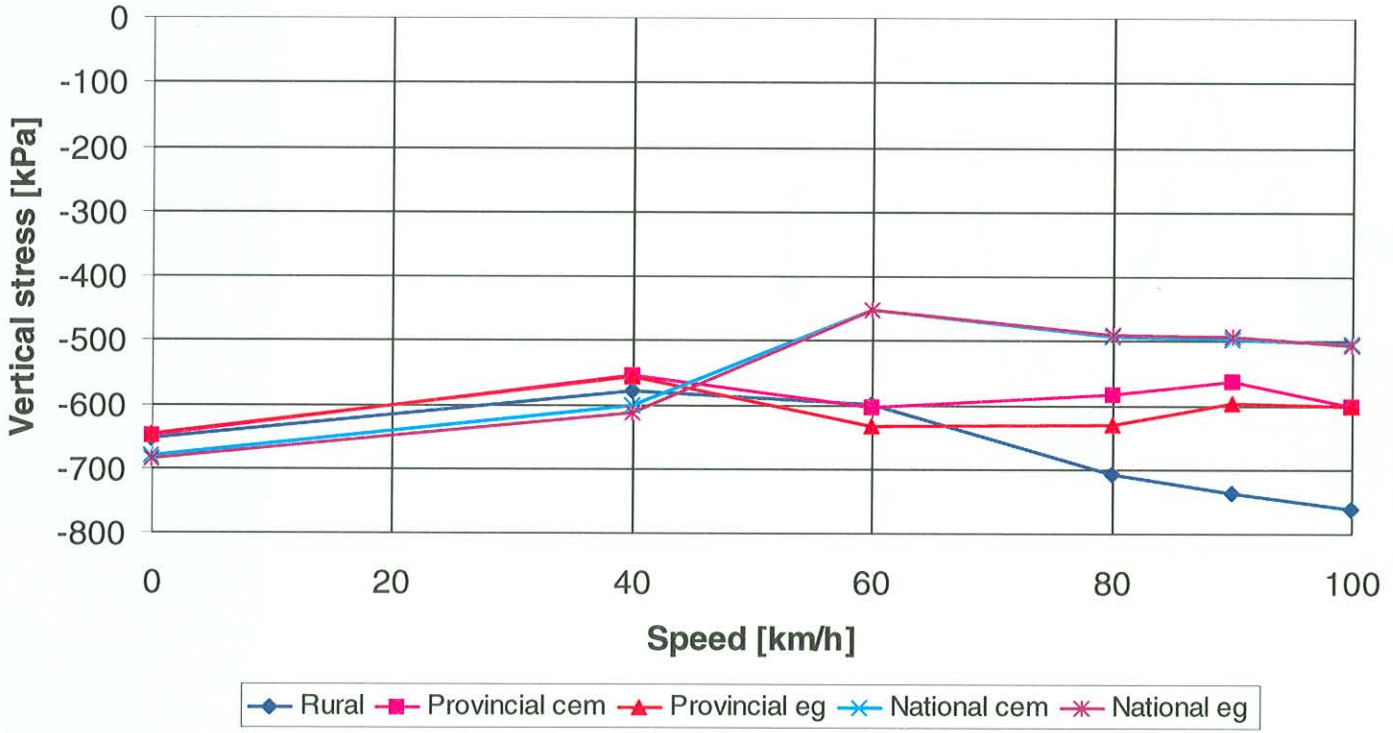

Figure 6.11: **Typical vertical stresses against speed (50th percentile load) as calculated using MCL method.**

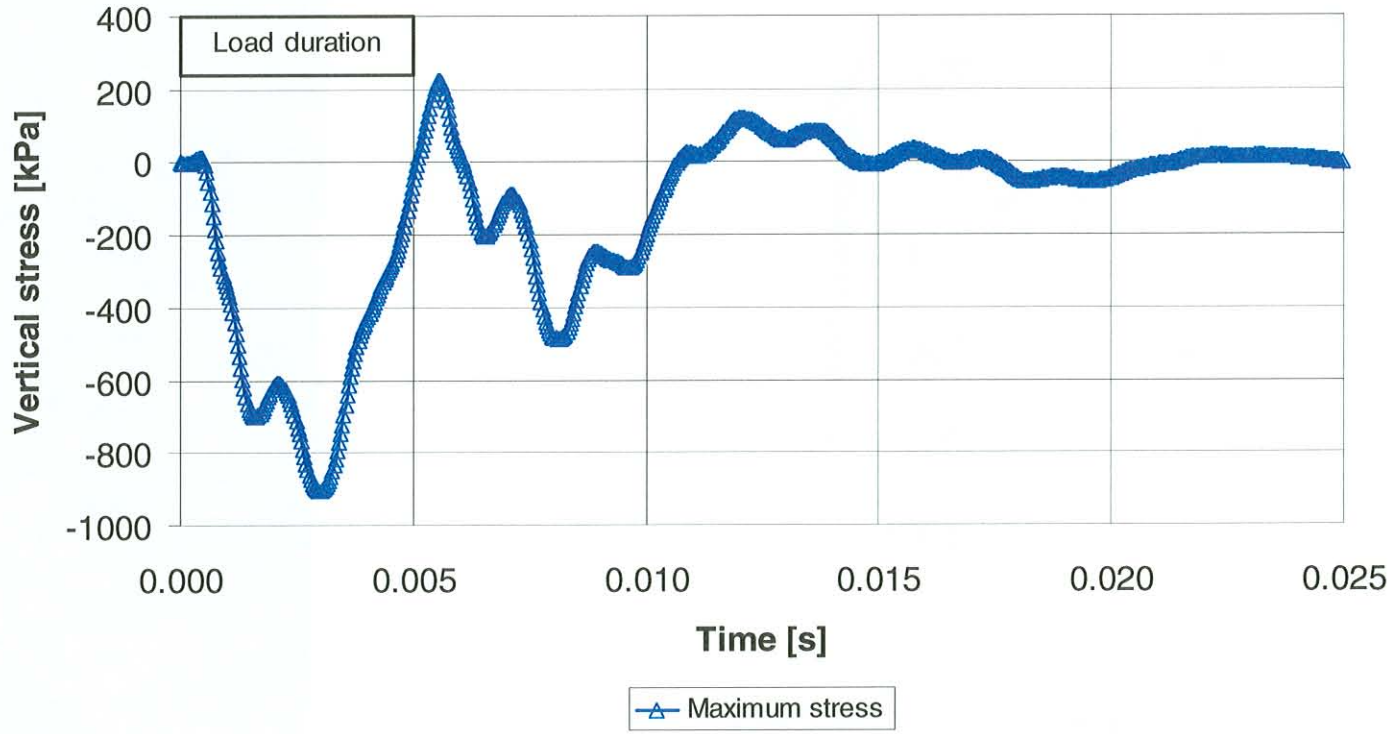

Figure 6.12: Typical vertical stresses (95th percentile load) as calculated using MCL method for rural pavement structure.

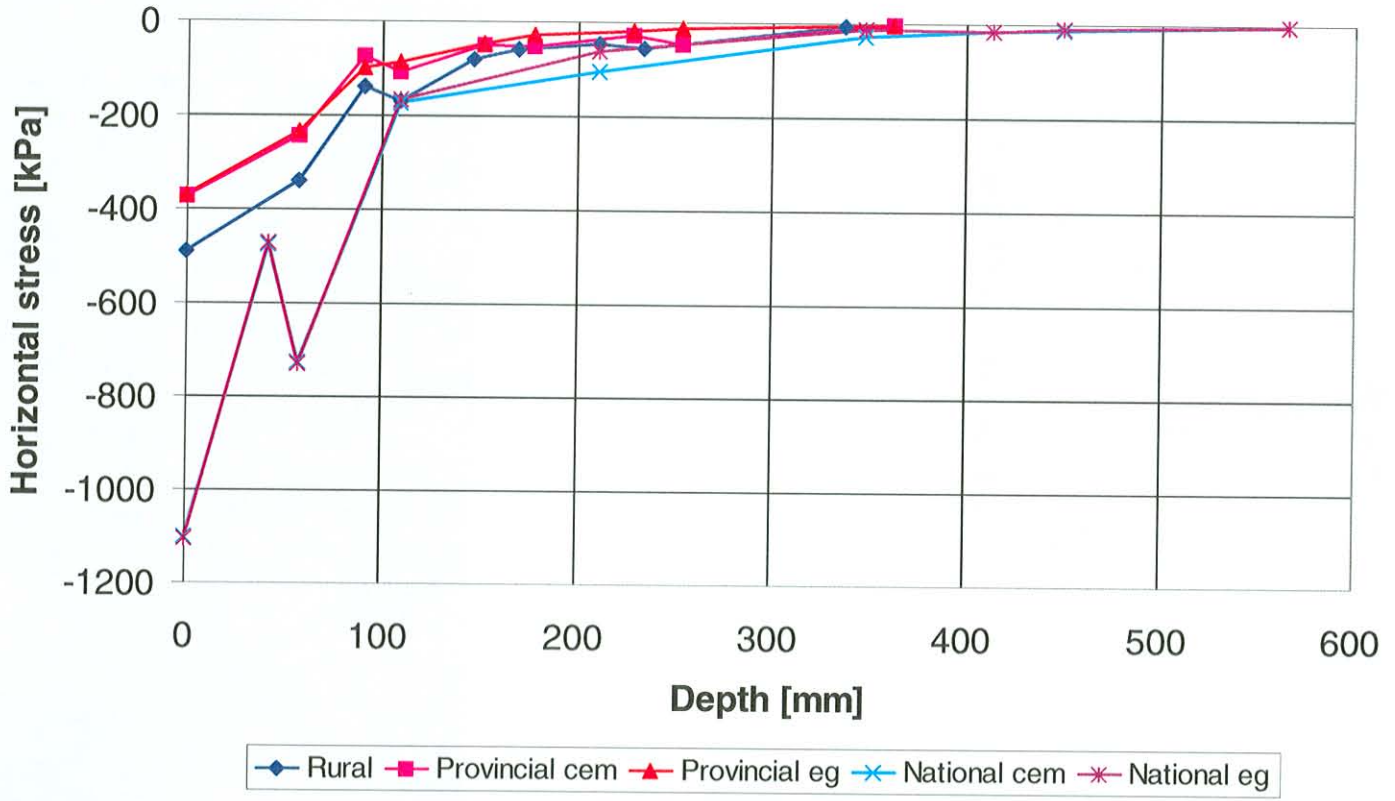

Figure 6.13: Typical horizontal stresses (50th percentile load) as calculated using the MCL method.

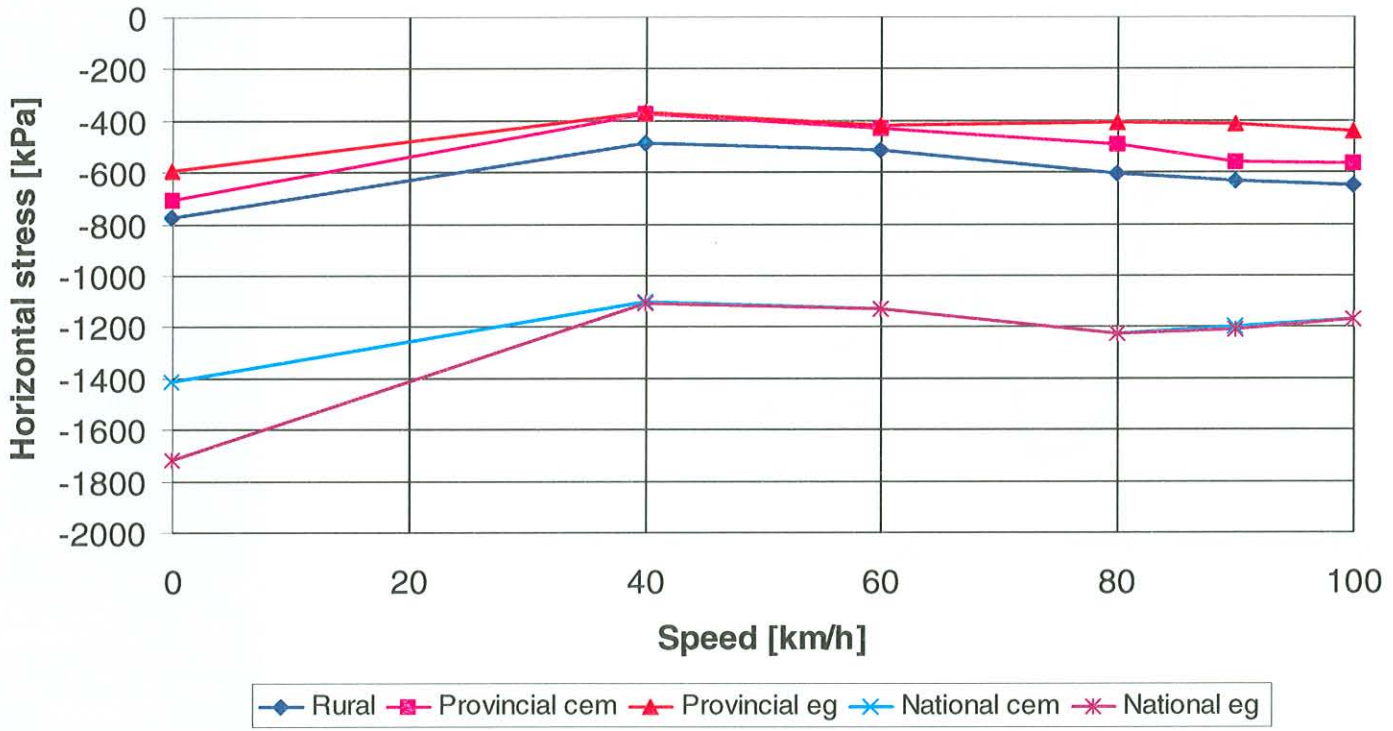

Figure 6.14: Typical horizontal stresses (50th percentile load) against speed as calculated using the MCL method.

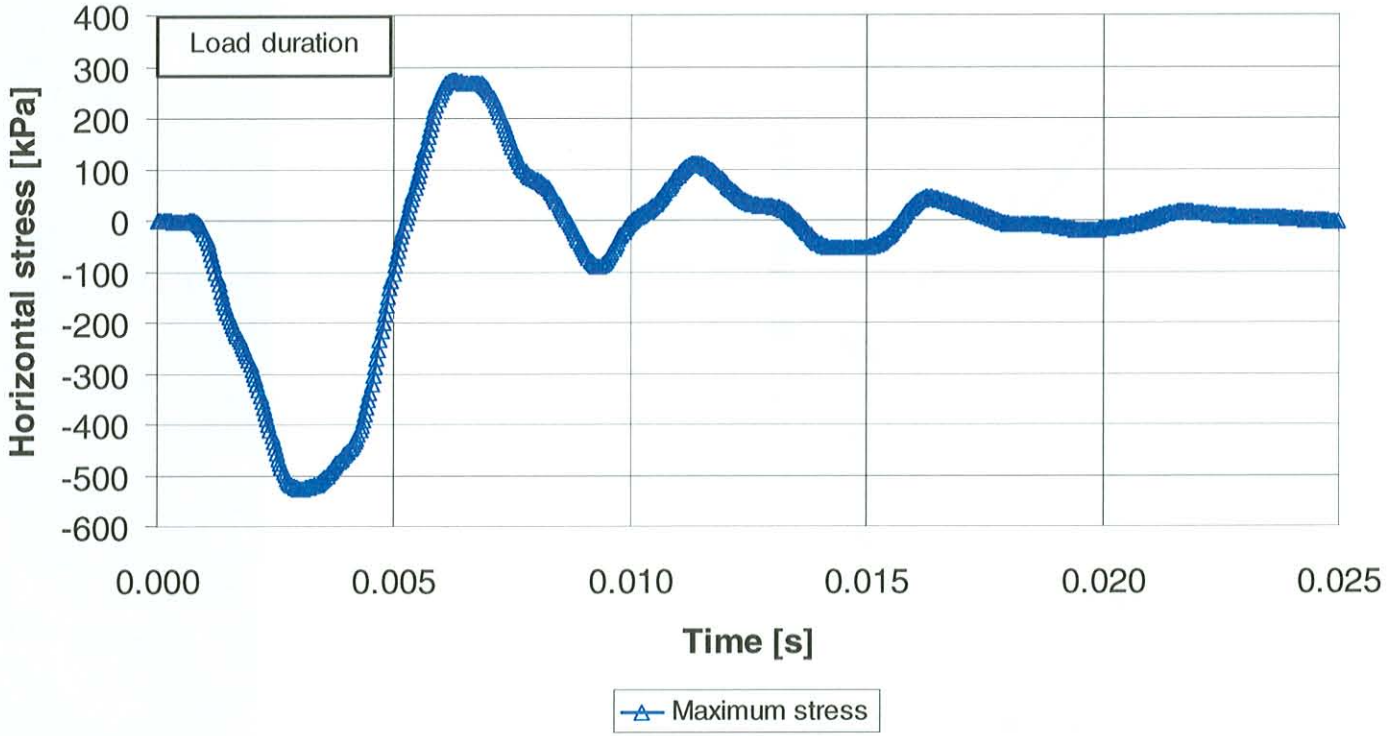

Figure 6.15: Typical horizontal stresses (95th percentile load) as calculated using the MCL method for a rural pavement structure.

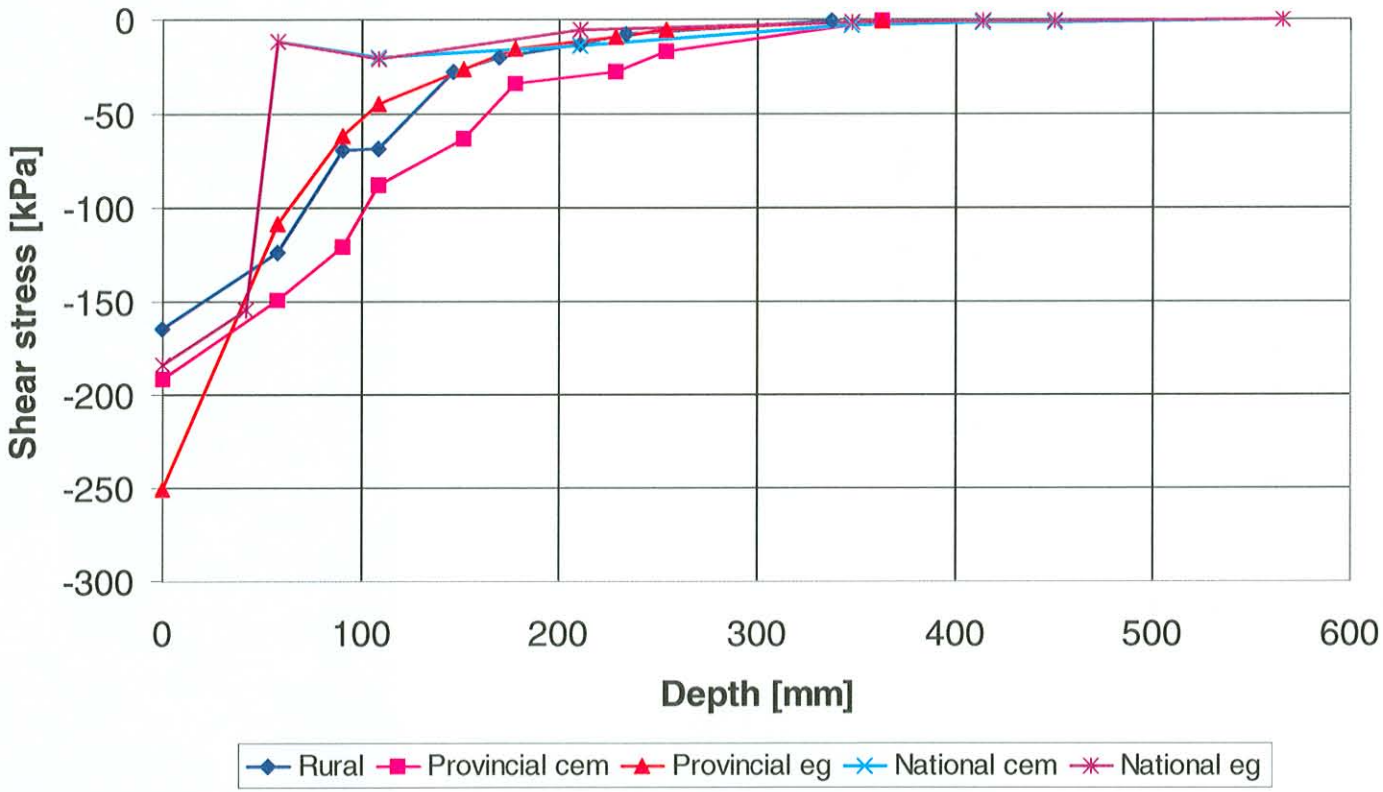

Figure 6.16: Typical shear stresses (50th percentile load) as calculated using the MCL method.

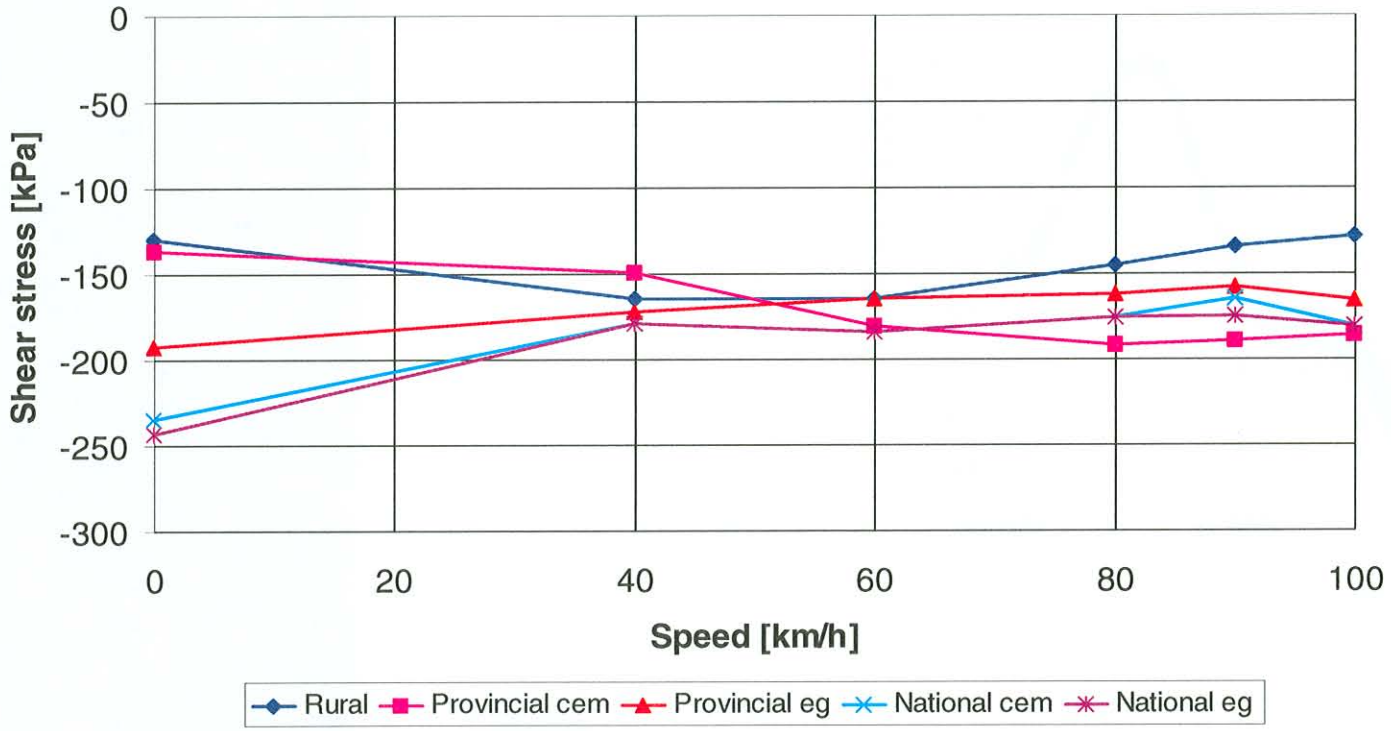

Figure 6.17: Typical shear stresses (50th percentile load) against speed as calculated using the MCL method.

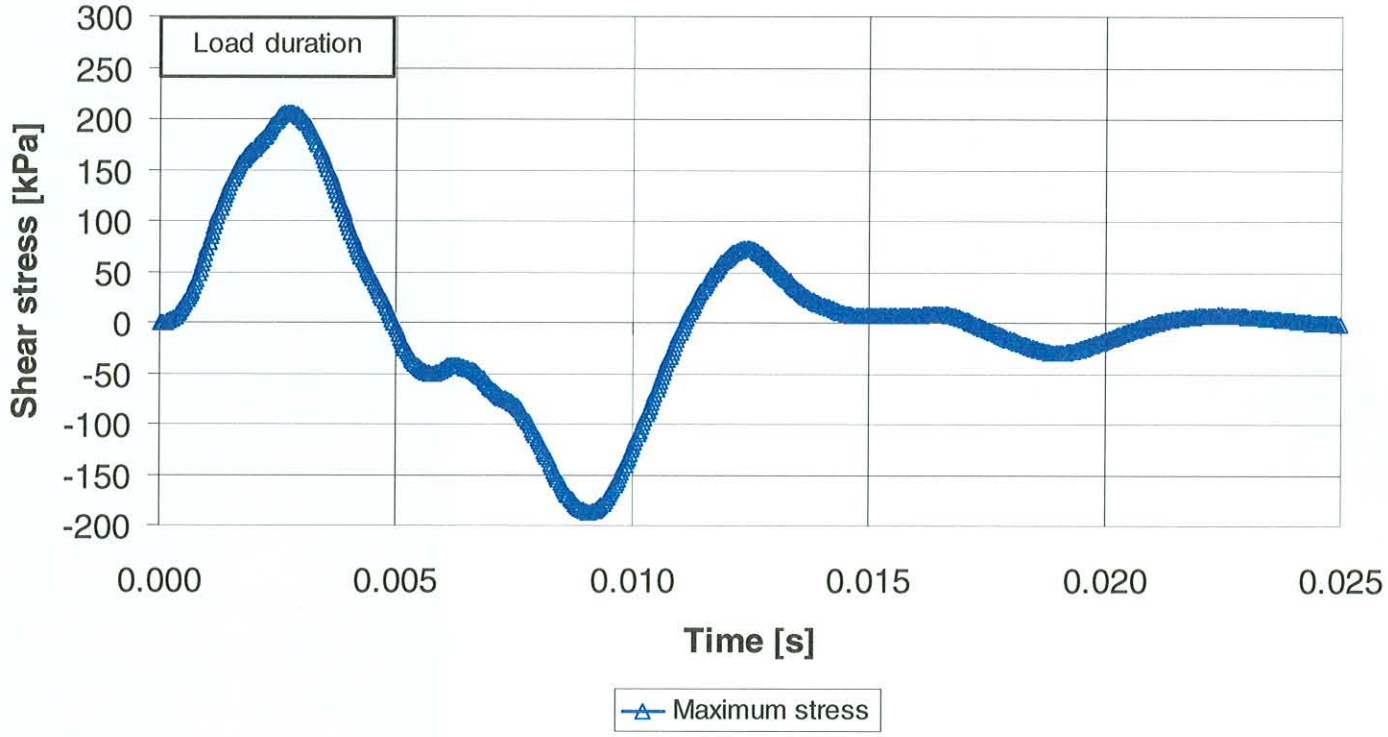

Figure 6.18: **Typical shear stresses (95th percentile load) as calculated using the MCL method.**

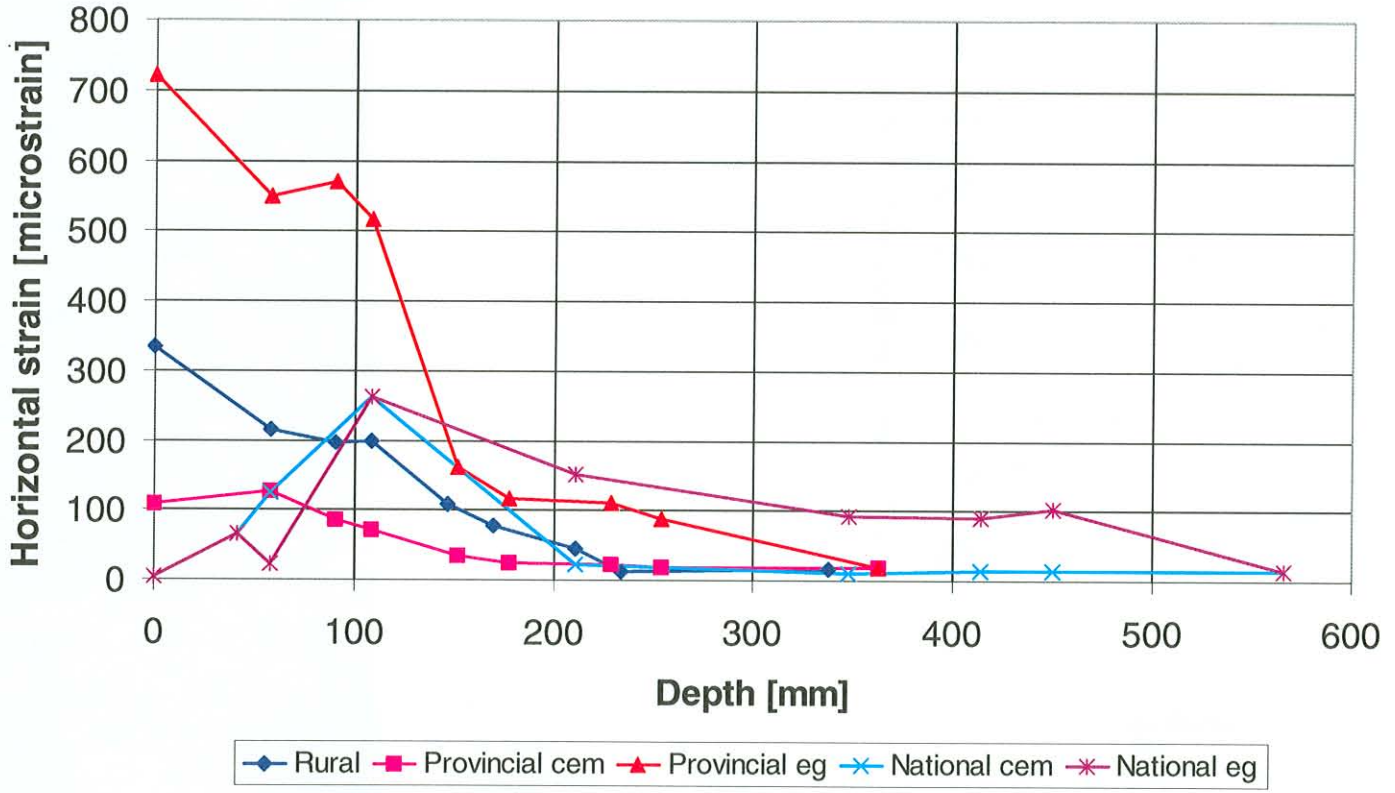

Figure 6.19: Typical horizontal tensile strain (50th percentile load) as calculated using the MCL method.

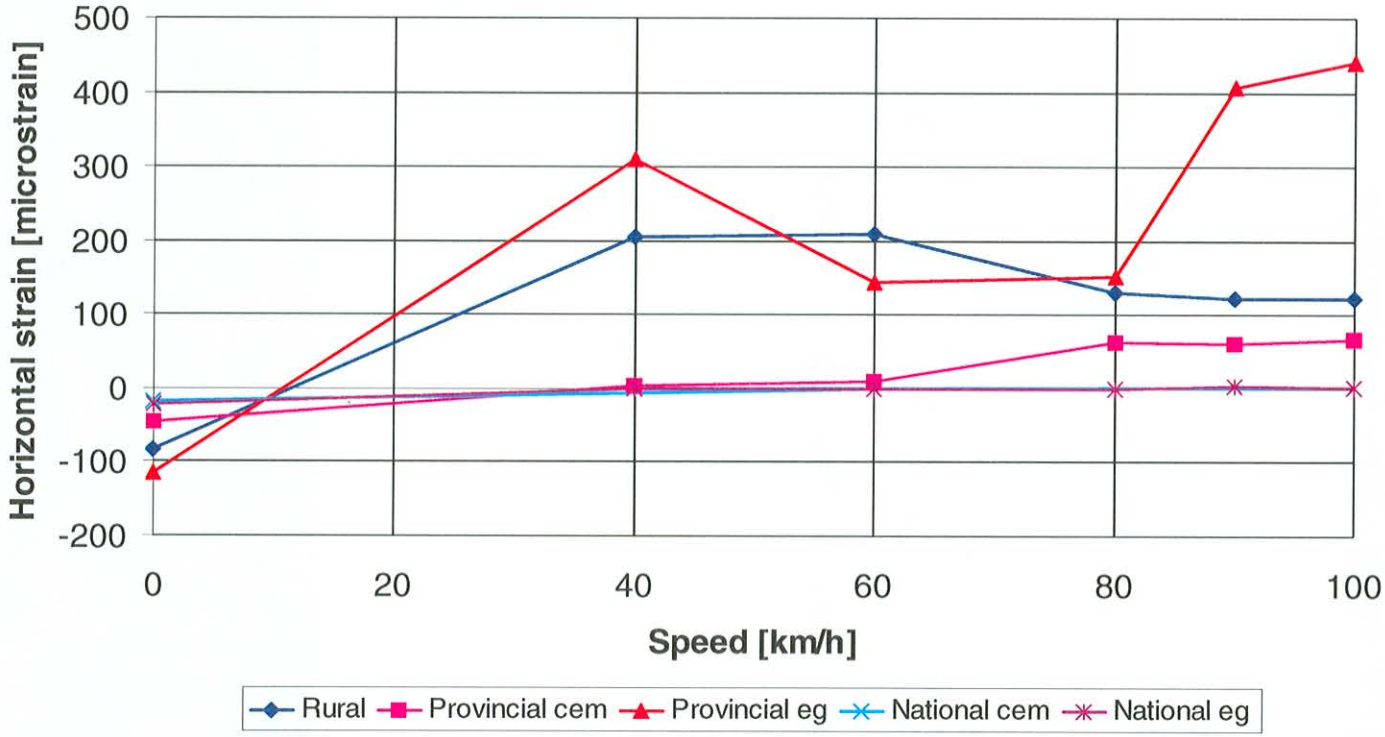

Figure 6.20: **Typical horizontal strain (50th percentile load) against speed as calculated using the MCL method.**

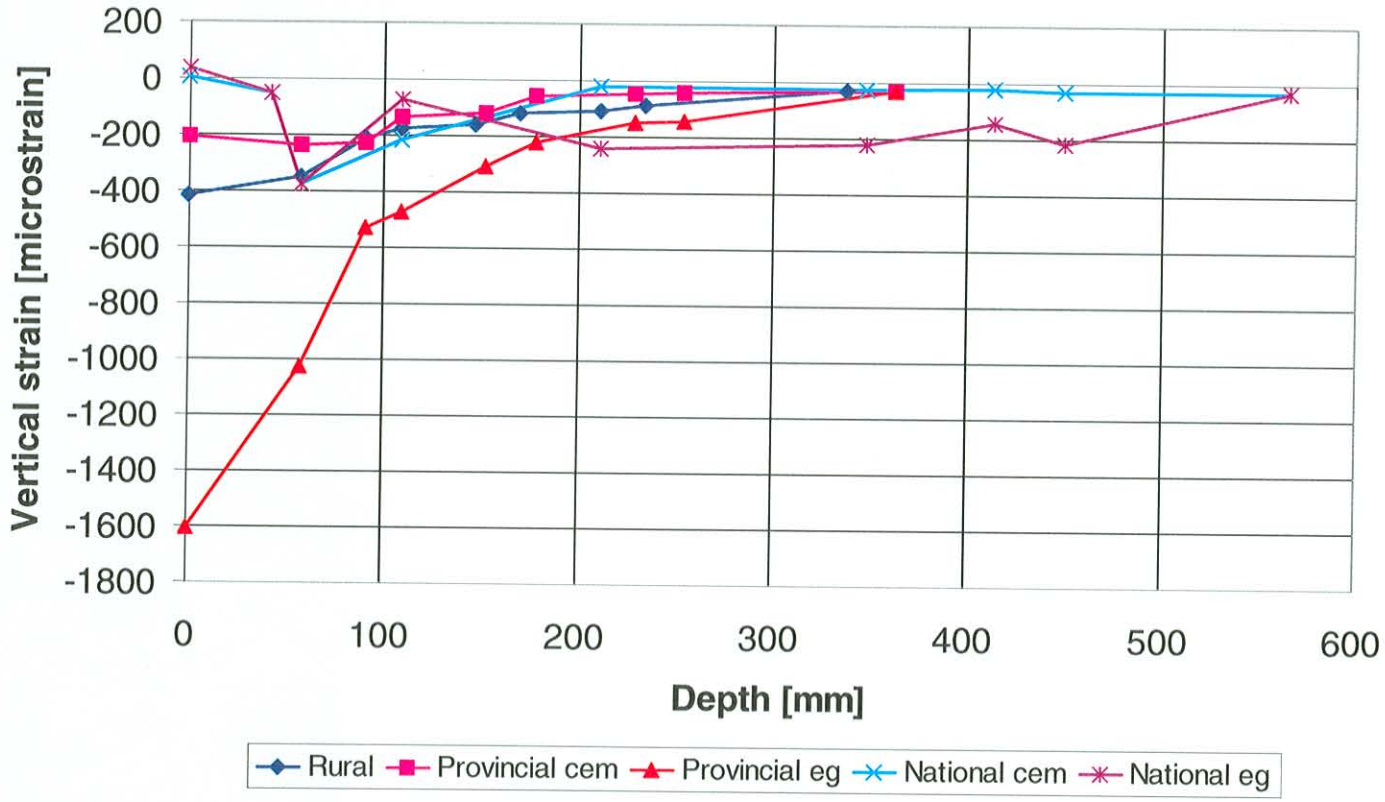

Figure 6.21: **Typical vertical compressive strain (50th percentile load) as calculated using the MCL method.**

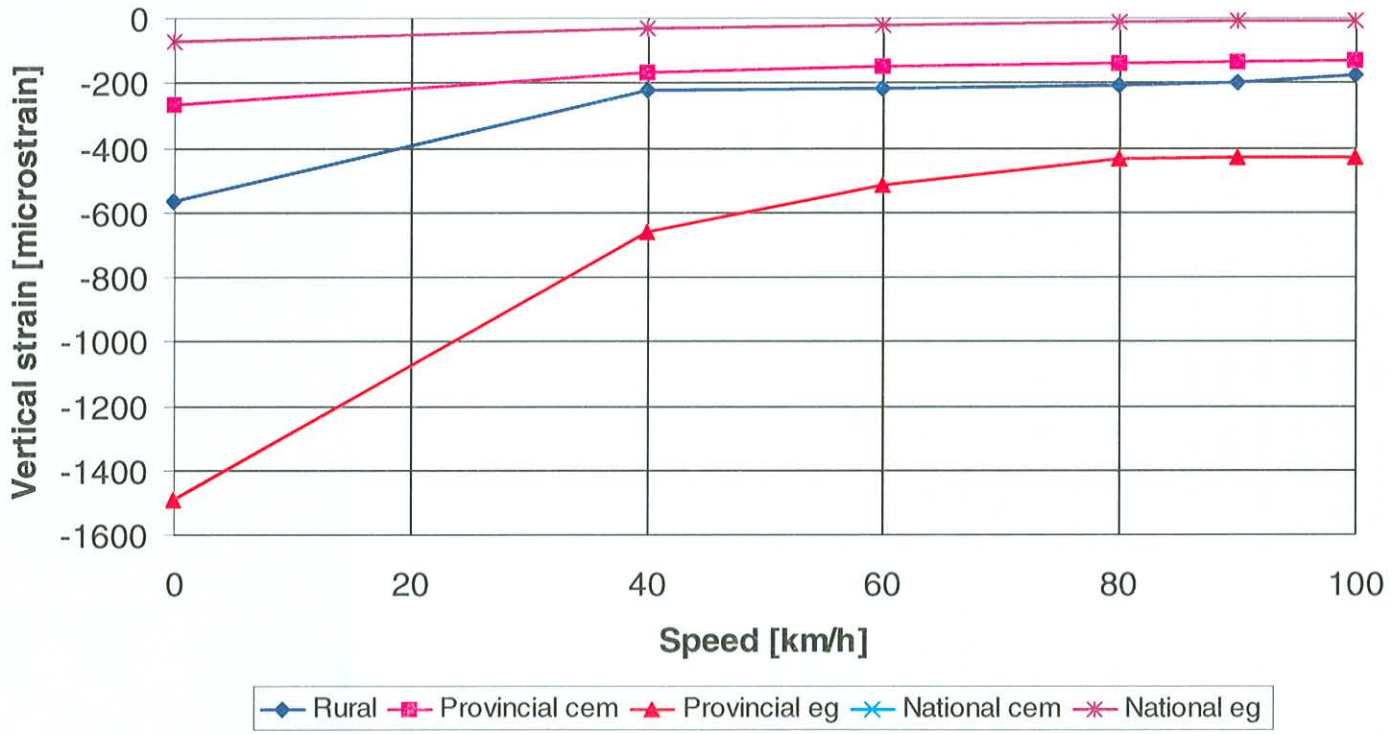

Figure 6.22: Typical vertical strain (50th percentile load) against speed as calculated using MCL method.

Statistical analyses

Statistical analyses were performed on the output from the MCL analyses to determine the factors that influence each of the pavement response parameters.

The first analysis was performed to determine the effect of load *magnitude* on the vertical and horizontal stresses and strains calculated. This analysis indicated relatively good relationships (R^2 > 75 per cent) between the vertical stress and load magnitude for most of the pavements at depths of less than 200 mm (exceptions being rural pavement surface, provincial ***eg*** pavement at middle of base layer and provincial ***cem*** pavement bottom of base layer). At deeper locations the relationships decreased to R^2 -values of below 40 per cent. A similar analysis on the relationships between the horizontal stresses and the load magnitude showed higher relationships in the upper layers (between 62 and 92 per cent) and these again decreased with increased depths. The relationships obtained were mostly (28 per cent) linear, followed by double reciprocal, log x, y-reciprocal, x-reciprocal and square root x relationships.

The relationships obtained between the vertical strain and the load magnitude were not good with R^2 –values of less than 50 per cent obtained for all the relationships. The relationships obtained between the horizontal strains and the load magnitude were nominally better than those obtained for the vertical strains, although the majority of the R^2 –values were still lower than 50 per cent.

The results of these analyses indicated that pavement response (in terms of vertical and horizontal stresses) in the upper layers of the pavement is highly correlated and dependent on the load magnitude. As the mass properties of the pavement structure are also included in a finite element analysis, it is probably the effects of these overburden stresses that cause the correlation between load magnitude and stress at the deeper layers to be lower than for the upper layers in the pavement. The fact that the load is spread out over a larger area at the deeper locations may also affect this correlation. The relationships between the load magnitude and strains (vertical and horizontal) are not correlated and these strains appear not to be affected by the load magnitude to a high degree. The few higher R^2- values obtained for the correlations between horizontal strains and load magnitude were all located in the upper part (base) of the respective pavements. The relationships between R^2- values and depth into the pavement for the five pavement structures are shown in Figure 6.23.

The second analysis was performed to determine the effect of load *speed* on the vertical and horizontal stresses and strains calculated. This analysis showed relationships (R^2- values) of less than 50 per cent for most (91 per cent) of the positions investigated in each of the pavements for the stress parameters. These relationships existed for all three stress parameters investigated, at all depths. The relationships obtained were mostly (40 per cent) linear, followed by y-reciprocal, x-reciprocal and double reciprocal relationships.

Strong relationships were obtained between the load speed and both the vertical and horizontal strains, with the majority of the R^2- values being between 60 and 90 per cent. The relationships between R^2- values and depth into the pavement for the five pavement structures are shown in Figure 6.24.

These results indicated that the pavement response stress parameters (vertical, horizontal and shear stresses) investigated are not related to the load speed to a high degree. However, the strain parameters (vertical and horizontal strains) relate to the load speed to a high degree.

It thus appears as if the stress components of the pavement response correlate mainly with the load *magnitude* while the strain components correlate with the load *speed*. A possible reason is the fact that due to Newton's law indicating that an applied force will be resisted by an equal force resisting in the opposite direction, the load applied to the pavement surface (and therefore stress) must be counteracted by an equal load (stress) to keep equilibrium. However, to develop strain in a body the effect of the applied load must first act on the whole body. If the body is resisting the effects of the applied load, the time for the strain effect to take place may cause strains to correlate better with load speed than load magnitude.

The third analysis consisted of a multiple regression between the pavement response parameters (vertical, horizontal and shear stresses) and the load magnitude and load speed. These analyses showed relationships with R^2- values of more than 80 per cent for all locations shallower than 150 mm in the pavement for all pavements except the provincial ***eg*** pavement's horizontal and vertical stresses. The correlations decreased with increasing depth. The obtained equations for the relationships between pavement response parameter and load magnitude and speed all showed negative slopes of between 8 and 18 for the load magnitude parameter, and between 0,4 and 1,1 for the speed parameter. This confirms the previous observation that the effect of the load magnitude is more pronounced than that of the load speed on the pavement stresses investigated.

The multiple regression relationships between the vertical and horizontal strains and the load magnitude and load speed yielded higher R^2- values in the base layers (R^2- values of 70 to 95 per cent). It again confirmed the previous observation that the strain is mostly affected by the load speed.

Analysis of the effect of load speed on the vertical elastic deflections indicated that relationships with R^2-values of higher than 99,8 per cent exist between the load speed and the vertical deflections for all the pavement structures.

The inference from these statistical relationships between load magnitude, load speed and pavement response parameters is that the load magnitude has a dominant effect on the calculated stresses, especially in the surfacing and base layers of the pavement, while the load speed has a dominant effect on the calculated strains and deflections in the pavement.

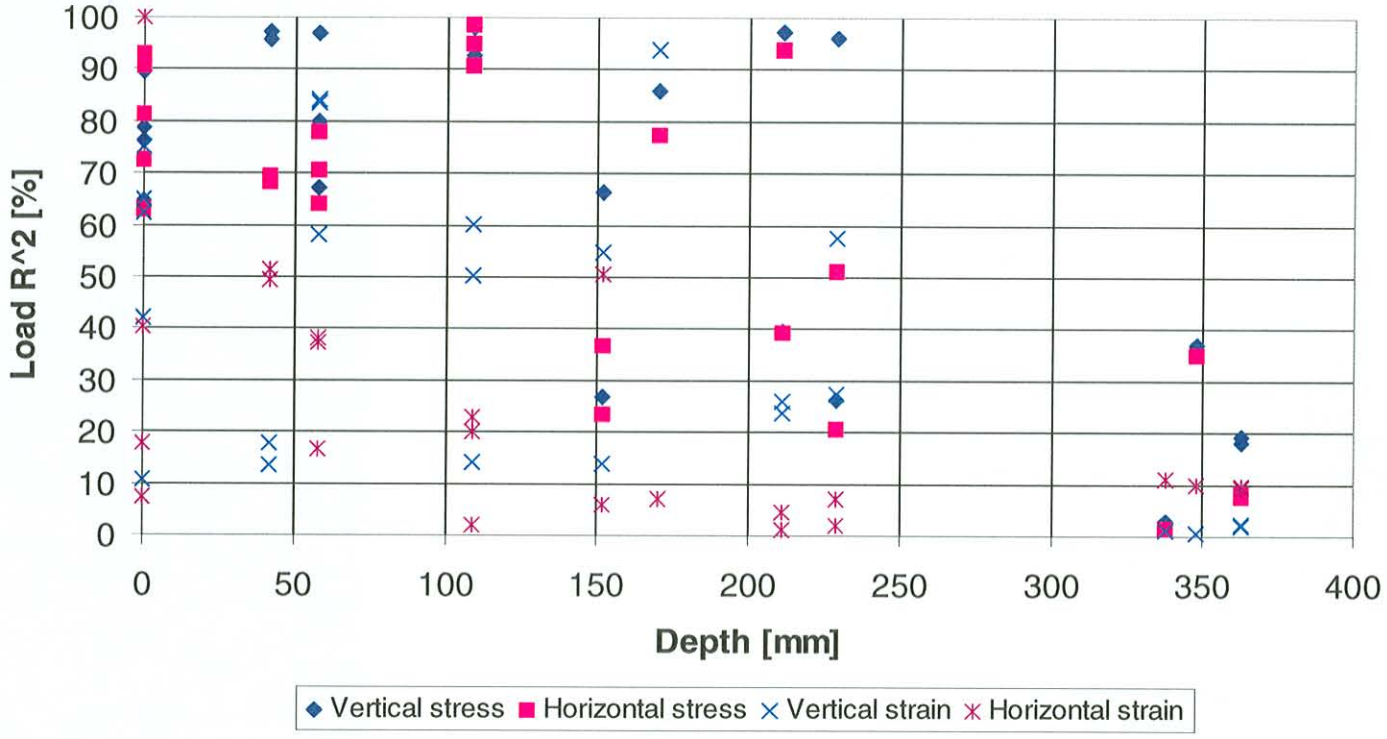

Figure 6.23: **Correlations obtained through statistical analysis of applied load magnitudes and calculated stresses.**

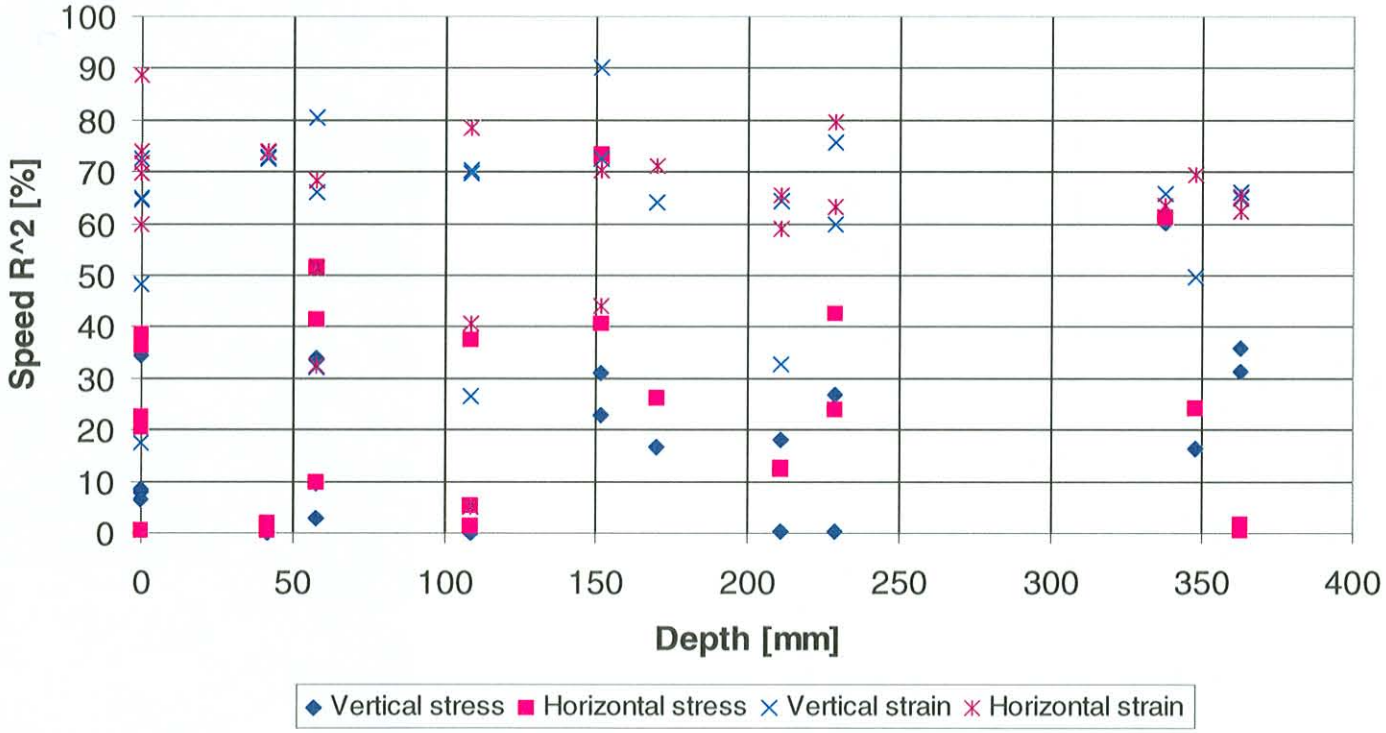

Figure 6.24: **Correlations obtained through statistical analysis of applied speed and calculated stresses.**

Effect of load frequency on pavement response parameters

It was previously (section 5.5) hypothesised that the effect of the higher frequency load variations (typical of the axle hop frequencies) have a more pronounced effect on the upper layers of the pavement structure than on the deeper levels. To test this hypothesis, analyses were performed where the same pavement structure was evaluated for the response to a load applied at a range of frequencies. The frequencies ranged from 1 Hz to 20 Hz, to extend wider than the typical scope of body bounce (around 3 Hz) and axle hop (around 18 Hz) frequencies.

It is important to distinguish between load speed and load frequency. In the previous sections the effect of load speed on pavement response parameters was investigated. Load speed is the physical horizontal speed at which the load moves along the pavement. Load frequency (which is specifically investigated in this section) indicates the rate at which the load magnitude varies with time. It is thus possible to have a tyre load with a high load speed and frequency or a low load speed and load frequency, or a combination of the two parameters.

For each of the analyses the displacements, stresses and strains were calculated for a period equal to the wavelength of the specific frequency. Typical load durations for the highway speeds used in this thesis, and a tyre patch of 300 mm, are between 0,0108 s (100 km/h) and 0,027 s (40 km/h). This represents load frequencies of between 92 and 37 Hz. It is thus realistic to expect that the calculated pavement responses for a period equal to the wavelength of the applied frequency would indicate the expected behaviour of the pavement. The first full wavelength for each load variation was used in the analyses.

To establish the effect of the load frequency on the pavement response, the ratio between the response at various depths in the pavement structure and at the surface was calculated at each of the frequencies evaluated. Using this ratio caused the response at the surface to always equal 1, and the responses at other depths to typically be less than one. These ratios provided dimensionless parameters to compare with each other. The ratios obtained for the different frequencies were then compared. The ratios were calculated using the 95^{th} percentile load data for each of the pavements used in this thesis.

If the ratios obtained at two frequencies are equal at a specific depth, it indicates that the specific response parameter is not influenced by the load frequency at that depth. If the ratio for frequency A at a specific depth is lower than the ratio for frequency B at the same depth, then the effect of frequency A is less at that specific depth than the effect of frequency B.

In Figure 6.25 the relationship between the calculated ratios for the 1Hz (low frequency) and 20 Hz (high frequency) frequencies for the surface elastic deflection are shown. A value of greater than 1 indicates that the higher frequency affects the pavement at the specific position less than the lower frequency. The data indicates that at distances of less than 0,5 m the effect of the higher frequency loads are less pronounced than that of the low frequency loads (all at the surface) for the rural and provincial (***cem*** and ***eg***) pavements. The same is true for the national pavement (***cem*** and ***eg***) at distances less than 0,75 m from the centre of the load. Further on the effects are similar, mainly due to the very small deflection responses calculated.

In Figure 6.26 the relationship between the calculated ratios for the 1Hz (low frequency) and 20 Hz (high frequency) frequencies for the vertical compressive stress are shown. The data indicates similar trends for the rural and provincial (***cem*** and ***eg***) pavements. All these pavements are not critically affected up to a depth of 250 mm, with the lower frequency affecting the pavements more at deeper levels. The national (***cem*** and ***eg***) pavements indicate at the surface (up to 100 mm) that the higher frequency affects the pavement more. This is probably due to the relatively stiff asphalt surfacing. The general trend from the national (***cem*** and ***eg***) pavements is to be affected more by the lower frequencies at lower depths.

In Figure 6.27 the relationship between the calculated ratios for the 1Hz (low frequency) and 20 Hz (high frequency) frequencies for the horizontal compressive stress are shown. The data indicates all the pavements to be more sensitive to the higher load frequency than the lower load frequency. This is especially true for the surfacing of the national ***cem*** pavement. At deeper depths the lower frequency starts to affect the pavement again more clearly.

In Figure 6.28 the relationship between the calculated ratios for the 1Hz (low frequency) and 20 Hz (high frequency) frequencies for the compressive shear stress are shown. The data indicates that all the pavements are more sensitive to the lower load frequency, except the surfacing (asphalt) of the national pavement.

In Figure 6.29 the relationship between the calculated ratios for the 1Hz (low frequency) and 20 Hz (high frequency) frequencies for the vertical compressive strain are shown. The data indicates that all the pavements are more sensitive to the lower load frequency with an increasing sensitivity at greater depths.

In Figure 6.30 the relationship between the calculated ratios for the 1Hz (low frequency) and 20 Hz (high frequency) frequencies for the horizontal tensile strain are shown. The data indicates that all the pavements are more sensitive to the lower load frequency with an increasing sensitivity at greater depths.